

## Disruption of the *Plasmodium falciparum* life cycle through transcriptional reprogramming by inhibitors of Jumonji demethylases

Krista A Matthews, Kossi M Senagbe, Christopher Notzel, Christopher A Gonzalez, Xinran Tong, Filipa Rijo-Ferreira, Bhana V Natarajan, Celia Miguel-Blanco, Maria Jose Lafuente-Monasterio, Benjamin A. Garcia, Bjorn FC Kafsack, and Elisabeth D. Martinez

*ACS Infect. Dis.*, **Just Accepted Manuscript** • DOI: 10.1021/acsinfecdis.9b00455 • Publication Date (Web): 09 Apr 2020

Downloaded from [pubs.acs.org](https://pubs.acs.org) on April 14, 2020

### Just Accepted

“Just Accepted” manuscripts have been peer-reviewed and accepted for publication. They are posted online prior to technical editing, formatting for publication and author proofing. The American Chemical Society provides “Just Accepted” as a service to the research community to expedite the dissemination of scientific material as soon as possible after acceptance. “Just Accepted” manuscripts appear in full in PDF format accompanied by an HTML abstract. “Just Accepted” manuscripts have been fully peer reviewed, but should not be considered the official version of record. They are citable by the Digital Object Identifier (DOI®). “Just Accepted” is an optional service offered to authors. Therefore, the “Just Accepted” Web site may not include all articles that will be published in the journal. After a manuscript is technically edited and formatted, it will be removed from the “Just Accepted” Web site and published as an ASAP article. Note that technical editing may introduce minor changes to the manuscript text and/or graphics which could affect content, and all legal disclaimers and ethical guidelines that apply to the journal pertain. ACS cannot be held responsible for errors or consequences arising from the use of information contained in these “Just Accepted” manuscripts.

1  
2  
3 **1 Disruption of the *Plasmodium falciparum* life cycle through transcriptional reprogramming**  
4 **2 by inhibitors of Jumonji demethylases**  
5  
6  
7 **3**  
8

9 4 Krista A. Matthews<sup>1</sup>, Kossi M. Senagbe<sup>2</sup>, Christopher Nötzel<sup>3,5</sup>, Christopher A. Gonzales<sup>2</sup>,  
10 5 Xinran Tong<sup>3</sup>, Filipa Rijo-Ferreira<sup>4</sup>, Bhanu V. Natarajan<sup>6</sup>, Celia Miguel-Blanco<sup>7</sup>, Maria Jose  
11 6 Lafuente-Monasterio<sup>7</sup>, Benjamin A. Garcia<sup>6</sup>, Björn F.C. Kafsack<sup>3,5</sup> and Elisabeth D.  
12 7 Martinez<sup>1,2,8,\*</sup>  
13  
14  
15 **8**  
16

17 9 <sup>1</sup> Department of Pharmacology, The University of Texas Southwestern Medical Center, 6000  
18 10 Harry Hines Blvd., Dallas, Texas, 75390 USA  
19

20 11 <sup>2</sup> Hamon Center for Therapeutic Oncology Research, The University of Texas Southwestern  
21 12 Medical Center, 6000 Harry Hines Blvd., Dallas, Texas, 75390 USA  
22  
23

24 13 <sup>3</sup> Department of Microbiology & Immunology, Weill Cornell Medicine, 1300 York Avenue, W-  
25 14 705, New York, New York, 10065 USA  
26

27 15 <sup>4</sup> Department of Neuroscience, The University of Texas Southwestern Medical Center, 6000  
28 16 Harry Hines Blvd., Dallas, Texas, 75390 USA  
29  
30

31 17 <sup>5</sup> Biochemistry, Cell & Molecular Biology Graduate Program, Weill Cornell Medicine, 1300  
32 18 York Avenue, W-705, New York, New York, 10065 USA  
33

34 19 <sup>6</sup> Epigenetics Program, Department of Biochemistry and Biophysics, Perelman School of  
35 20 Medicine, University of Pennsylvania, 3400 Civic Center Blvd., Bldg. 421, Philadelphia,  
36 21 Pennsylvania, 19104 USA  
37  
38

39 22 <sup>7</sup> GlaxoSmithKline, Tres Cantos Medicines Development Campus, Tres Cantos, P.T.M Severo  
40 23 Ochoa, Madrid, 28760 Spain  
41

42 24 <sup>8</sup> Lead contact  
43

44  
45 25 \*correspondence to: [elisabeth.martinez@utsouthwestern.edu](mailto:elisabeth.martinez@utsouthwestern.edu)  
46  
47  
48

49 27 Running title: Effect of mammalian Jumonji KDM inhibitors on malaria  
50  
51  
52  
53  
54  
55  
56  
57  
58  
59  
60

1  
2  
3 **28 Abstract**  
4  
5

6 29 Little is known about the role of the three Jumonji C (JmjC) enzymes in *Plasmodium falciparum*  
7  
8 30 (*Pf*). Here we show that JIB-04 and other established inhibitors of mammalian JmjC histone  
9  
10 31 demethylases kill asexual blood stage parasites and are even more potent at blocking gametocyte  
11  
12 32 development and gamete formation. In late stage parasites, JIB-04 increased levels of tri-  
13  
14 33 methylated lysine residues on histones suggesting inhibition of *P. falciparum* Jumonji demethylase  
15  
16 34 activity. These epigenetic defects coincide with deregulation of invasion, cell motor, and sexual  
17  
18 35 development gene programs, including gene targets coregulated by the PfAP2-I transcription  
19  
20 36 factor and chromatin-binding factor, PfBDP1. Mechanistically, we demonstrate that PfJmj3  
21  
22 37 converts 2-oxoglutarate to succinate in an iron-dependent manner consistent with mammalian  
23  
24 38 Jumonji enzymes, and this catalytic activity is inhibited by JIB-04 and other Jumonji inhibitors.  
25  
26 39 Our pharmacological studies of Jumonji activity in the malaria parasite provides evidence that  
27  
28 40 inhibition of these enzymatic activities is detrimental to the parasite.  
29  
30  
31  
32  
33  
34  
35  
36  
37

38 41  
39  
40 42 Keywords: malaria, *Plasmodium falciparum*, demethylases, Jumonji inhibitors, JIB-04,  
41  
42 43 transcriptional reprogramming, gametocytes  
43  
44  
45  
46  
47  
48  
49  
50  
51  
52  
53  
54  
55  
56  
57  
58  
59  
60

## 44 Introduction

45 *Plasmodium falciparum* (*Pf*) is the most lethal of the five species of malaria affecting 3.4 billion  
46 humans annually <sup>1</sup>. The *P. falciparum* life cycle consists of single rounds of replication in the  
47 mosquito and human liver followed by the release of merozoites into the blood stream. Following  
48 red blood cell (RBC) invasion by the extracellular merozoites, the asexual blood stages initiate  
49 remodeling of their host cell (ring forms and early trophozoite) followed by repeated rounds of  
50 nuclear replication (late trophozoite/early schizont) and a single round of cell division (schizont)  
51 ending with the release of new merozoites from the infected RBC 48 h later. A low percentage of  
52 schizonts form merozoites that are committed to differentiate into male and female sexual stage  
53 gametocytes that mediate transmission to the next host. Proper transcriptional regulation at each  
54 stage of *P. falciparum* development is essential for the successful completion of the life cycle <sup>2</sup>. *P.*  
55 *falciparum* controls several key gene expression programs through epigenetic mechanisms  
56 mediated by histone modifying enzymes. The tri-methylation of histones at specific genomic loci  
57 regulates the expression of stage-specific transcription factors such as AP2-G, of nutrient uptake  
58 channels including the *clag3* gene paralogs, of invasion pathways, and of multi-gene families  
59 involved in antigenic variation <sup>2-11</sup>.

60 Histone tri-methylation is regulated by tri-methyl writers (including SET enzymes) and tri-  
61 methyl erasers. Jumonji C domain (JmjC) containing enzymes, a subfamily of 2-oxoglutarate (2-  
62 OG)-dependent oxygenases that catalyze hydroxylation and demethylation of substrates, are the  
63 known demethylases of histone tri-methylation (reviewed in <sup>12</sup>). The core of the JmjC domain is  
64 comprised of a double-stranded  $\beta$ -helix fold containing the active site residues that coordinate  
65 Fe(II), bind 2-OG, and interact with substrates like histone tails <sup>12-13</sup>. The binding of Fe(II) and 2-  
66 OG initiates the oxidative decarboxylation of 2-OG, generating succinate and an iron intermediate.

1  
2  
3 67 Jumonji enzymes use this intermediate to either hydroxylate or demethylate a variety of protein  
4  
5 68 and non-protein substrates. In contrast to the large family of Jumonji enzymes in mammals (~30),  
6  
7 69 the *P. falciparum* genome encodes only three proteins containing JmjC enzymatic domains,  
8  
9 70 designated as PfJmjC1 (PF3D7\_080990), PfJmjC2 (PF3D7\_0602800), and PfJmj3  
10  
11 (PF3D7\_1122200)<sup>14-15</sup>. The catalytic triad residues that coordinate Fe(II) (HxD/E,H) and the 2-  
12  
13 71 OG-binding residues are conserved in all three *P. falciparum* proteins. Furthermore, all three *P.*  
14  
15 72 *falciparum* Jumonji enzymes are expressed during the parasite's intraerythrocytic developmental  
16  
17 73 cycle (IDC), gametocyte development, and in ookinetes<sup>16-19</sup>. Jiang *et al.* generated single knockout  
18  
19 74 lines of PfJmjC1 and PfJmjC2 that were viable, indicating that neither of these enzymes are  
20  
21 75 essential for blood stage parasite survival in a laboratory environment<sup>15</sup>. PfJmj3 has yet to be  
22  
23 76 subjected to similar knockout analysis, although a recent transposon mutagenesis study suggests  
24  
25 77 that an exonal insertion in the gene for PfJmj3 yields viable parasites<sup>20</sup>. The essentiality of the  
26  
27 78 Jumonji enzymes in other stages of *P. falciparum*'s life cycle has yet to be investigated. In all  
28  
29 79 organisms studied to date, Jumonji histone lysine demethylases (KDMs) are the only family of  
30  
31 80 histone demethylases enzymatically capable of removing tri-methyl marks, thus the aggregate  
32  
33 81 PfJmj histone demethylase activity is likely central in regulating transcriptional programs in the  
34  
35 82 parasite<sup>12,21</sup>.  
36  
37  
38  
39  
40  
41  
42

43 84 We and others have developed small molecule inhibitors of mammalian Jumonji KDM  
44  
45 85 enzymes which interfere with catalysis by disrupting interactions with the iron cofactor, the 2-OG  
46  
47 86 co-substrate, and/or the histone substrate<sup>22-29</sup>. Since PfJmj proteins contain the conserved amino  
48  
49 87 acid residues for binding to co-factor, co-substrate, and substrate, we speculated that these  
50  
51 88 inhibitors would block the total Jumonji catalytic activity in the parasite. We therefore evaluated  
52  
53 89 the antimalarial activity of a collection of small molecule inhibitors of mammalian Jumonji KDM  
54  
55  
56  
57  
58  
59  
60

1  
2  
3 90 enzymes with a range of specificities against various subfamilies. We find that inhibitors of  
4  
5 91 mammalian Jumonji KDMs arrest parasite development and trigger parasite death in replicating  
6  
7  
8 92 blood stages, and potently prevent gametocyte development and gamete formation. Furthermore,  
9  
10 93 we show that three of the four small molecules inhibit conversion of 2-OG to succinate by  
11  
12 94 recombinant PfJmj3. Consistent with inhibition of malarial Jumonji KDMs, Jumonji inhibitors  
13  
14 95 alter global levels of histone tri-methylation in *P. falciparum*, resulting in deregulation of the  
15  
16  
17 96 parasite's transcriptional developmental program and ultimately parasite death.  
18  
19  
20  
21  
22  
23  
24  
25  
26  
27  
28  
29  
30  
31  
32  
33  
34  
35  
36  
37  
38  
39  
40  
41  
42  
43  
44  
45  
46  
47  
48  
49  
50  
51  
52  
53  
54  
55  
56  
57  
58  
59  
60

## 97 **Results**

### 98 *Inhibitors of mammalian Jumonji enzymes have antimalarial activity against drug sensitive and* 99 *drug resistant asexual blood stage parasites in culture*

100 The *Plasmodium falciparum* (*Pf*) genome encodes three proteins containing JmjC enzymatic  
101 domains, designated as PfJmjC1 (PF3D7\_080990), PfJmjC2 (PF3D7\_0602800), and PfJmj3  
102 (PF3D7\_1122200) (Figure S1A). Residues in the mammalian Jumonji enzymes that are required  
103 for catalysis through iron and 2-oxoglutarate (2-OG) binding and for substrate binding are  
104 conserved in all three *P. falciparum* proteins (Figure S1B). Since several known inhibitors of  
105 mammalian Jumonji enzyme activity interfere with iron/2-OG/substrate binding, we evaluated  
106 these small molecules for antimalarial activity<sup>22-29</sup>. We first tested our own pan-selective inhibitor  
107 of Jumonji KDMs, JIB-04, in its active (E) and inactive (Z) isomeric forms since it is potent in  
108 culture and active *in vivo* against KDMs in cancer mammalian models (Table S1)<sup>23</sup>. We measured  
109 inhibition of blood stage asexual parasite growth using a standard 3-day assay in parasites  
110 synchronized to rings<sup>30</sup>. JIB-04 E isomer blocked the viability of both drug-sensitive 3D7 as well  
111 as multidrug-resistant Dd2 parasites with an EC<sub>50</sub> of 1.6 μM, while the inactive Z isomer was far  
112 less effective (EC<sub>50</sub> > 10 μM) (Figure 1A, left panel, and Figure S1C). To establish the generality  
113 of these findings, we then tested a panel of other known Jumonji inhibitors with various  
114 specificities for the mammalian enzymes (Table S1). GSK-J4, which preferentially inhibits  
115 H3K27me3 Jumonji KDMs in some model systems also inhibited both 3D7 and Dd2 parasites  
116 while the less active isomer GSK-J5 did not (Figure 1A, right panel, and Figure S1C-D)<sup>23, 27, 31-33</sup>.  
117 ML324 and SD-70, reported to inhibit KMD4 Jumonji family members, were also active against  
118 3D7 and Dd2 parasites (Figure 1A, right panel and S1D)<sup>34-35</sup>. Inhibitors known to selectively  
119 target the KDM5 subfamily of Jumonji enzymes such as CPI-455 and KDM5-C70 lacked

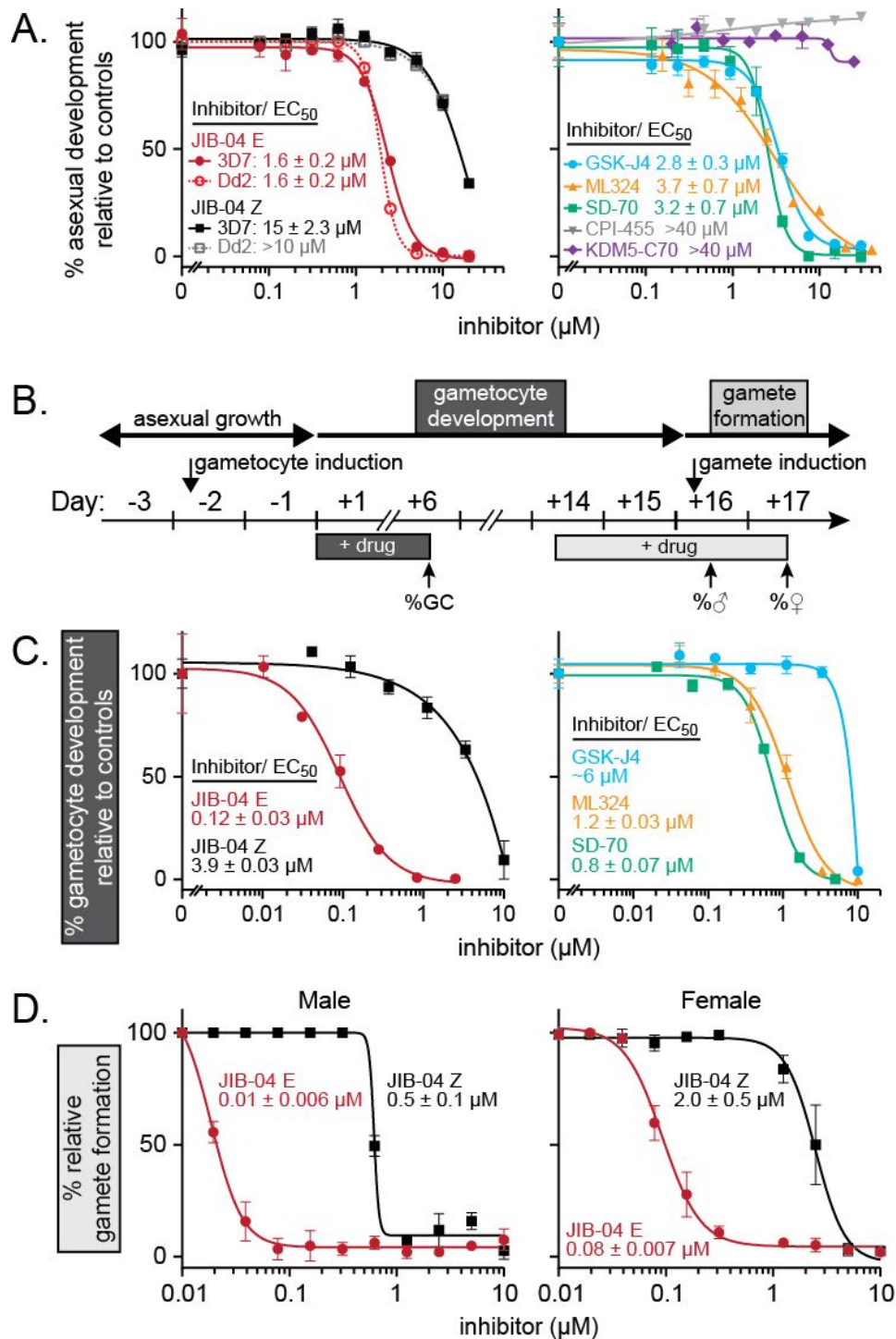


**Figure 1. Jumonji inhibitors are active against asexual erythrocytic growth and potentially block Pf gametocyte development and gamete formation**

Representative Jumonji inhibitor concentration curves against A) asexual development, C) gametocyte development, and D) gamete formation. A) 3D7 (solid line) or Dd2 (dashed line) asexual parasites synchronized to rings were treated with JIB-04 E (red circles) and Z (black squares) isomers (left panel), or GSK-J4 (cyan circles), ML324 (orange triangles), SD-70 (green squares), CPI-455 (grey inverted triangles), and KDM5-C70 (purple diamonds) (right panel).

120

**Figure 1 cont.** Asexual development was measured using the standard 3-day growth assay as described in Methods and is presented as a percent of vehicle-treated controls. B) Schematic of gametocyte and gamete induction relative to inhibitor exposure. Synchronized asexual parasites were cultured at high parasitemia on Day -2 to induce gametocytogenesis. For development assays (dark grey boxes), gametocytes were exposed to inhibitor starting on day +1 through to day +6. Parasitemia (%PT) and gametocytemia (%GC) were measured by flow cytometry as described in the Methods. For gamete formation assays (light grey boxes), inhibitor was added to stage V gametocytes for 48 h prior to induction on day +14. Male exflagellation (%♂) and female gamete formation (%♀) was measured on day +16 and day +17, respectively, as described in the Methods. C) Representative concentration curves of JIB-04 E and Z (left panel) and other Jumonji inhibitors (right panel) against gametocyte development relative to vehicle controls. D) Representative concentration curves of JIB-04 E and Z against male (left panel) and female (right panel) gamete formation relative to vehicle controls. Non-linear regression curves ([Inhibitor] vs. response - Variable slope (four parameters)) were fit to the data using GraphPad Prism v8. Error bars represent the standard deviation of technical triplicates. EC<sub>50</sub> concentrations (μM) are presented as mean ± SEM of the fitted inhibition curves from three or more independent experiments.

121 antimalarial activity even at the highest doses tested (40 μM) (Figure 1A, right panel) <sup>26, 29, 36</sup>.

123 Inhibition by JIB-04 E, GSK-J4, ML324, and SD-70, but not by CPI-455 or KDM5-C70, all active  
124 site inhibitors, suggests that effects on parasite growth are specific and not simply the result of  
125 general iron chelation or cytotoxicity against RBCs. Taken together, these studies establish that  
126 multiple Jumonji KDM inhibitors targeting mammalian enzymes other than only KDM5s are  
127 effective at blocking the viability of both drug-sensitive and drug-resistant blood stage *P.*  
128 *falciparum* parasites with similar potency.

### 129 ***Jumonji inhibitors disrupt gametocyte development and gamete formation***

130 Next we investigated the effects of Jumonji inhibitors on gametocyte (GC) development.  
131 Following sexual commitment, re-invaded ring stages were exposed to N-acetylglucosamine to  
132 kill asexual parasites and to Jumonji inhibitors for six days. Gametocytotemia was quantified by  
133 flow cytometry on day 6 (%GC) (Figure 1B; gametocyte development). JIB-04 E was highly  
134 effective in preventing gametocyte development as were SD-70 and ML324. Dose response studies  
135 determined that among these Jumonji inhibitors, JIB-04 E is the most potent inhibitor of

1  
2  
3 136 gametocyte development with an EC<sub>50</sub> concentration of ~120 nM, followed by SD-70 (~800 nM)  
4  
5 137 and ML324 (~1 μM) (Figure 1C). GSK-J4 and the inactive Z isomer of JIB-04 were effective only  
6  
7  
8 138 at high doses (Figure 1C). Thus while JIB-04, SD-70 and ML324 have 4-12 fold higher potency  
9  
10 139 against these sexual stages than against asexual parasites, GSK-J4 loses potency.

11  
12  
13 140 We then assessed if JIB-04 had effects on gamete maturation using the dual gamete  
14  
15 141 formation assay (Figure 1B; gamete formation)<sup>37-38</sup>. We measured male gamete formation by  
16  
17 142 exflagellation assays and female gamete formation by live cell staining with anti-Pfs25-Cy3  
18  
19 143 antibodies, a female-gamete specific marker<sup>39</sup>. JIB-04 E potently inhibited male exflagellation  
20  
21 144 centers with an EC<sub>50</sub> of ~10 nM while the inactive Z isomer had a much weaker effect (>500 nM)  
22  
23 145 (Figure 1D, left panel). JIB-04 E also robustly blocked female gamete formation as measured by  
24  
25 146 decreased Pfs25 protein, with EC<sub>50</sub> values of ~80 nM compared to >2 μM for inactive Z isomer  
26  
27 147 (Figure 1D, right panel). These results indicate that Jumonji inhibitors disrupt gametocyte  
28  
29 148 development and gamete formation with high potency preferentially blocking male gamete  
30  
31 149 formation.

### 32 33 34 35 36 37 150 **Jumonji inhibitors delay progression of ring- or trophozoite-treated asexual blood stage** 38 39 151 **parasites**

40  
41  
42 152 To further characterize the mode of antimalarial action of Jumonji inhibitors, we treated parasites  
43  
44 153 synchronized at specific blood form stages and evaluated the effects of drug exposure on  
45  
46 154 subsequent progression through the intraerythrocytic developmental cycle (IDC). First, we treated  
47  
48 155 rings with each inhibitor at its EC<sub>50</sub> concentration and monitored parasite development 24 h and  
49  
50 156 48 h post exposure by flow cytometry (Figures 2A-B and S2A-B). After 24 h, about 65% of rings  
51  
52 157 treated with vehicle had progressed to trophozoites and 15% to schizonts (Figures 2A and S2A).

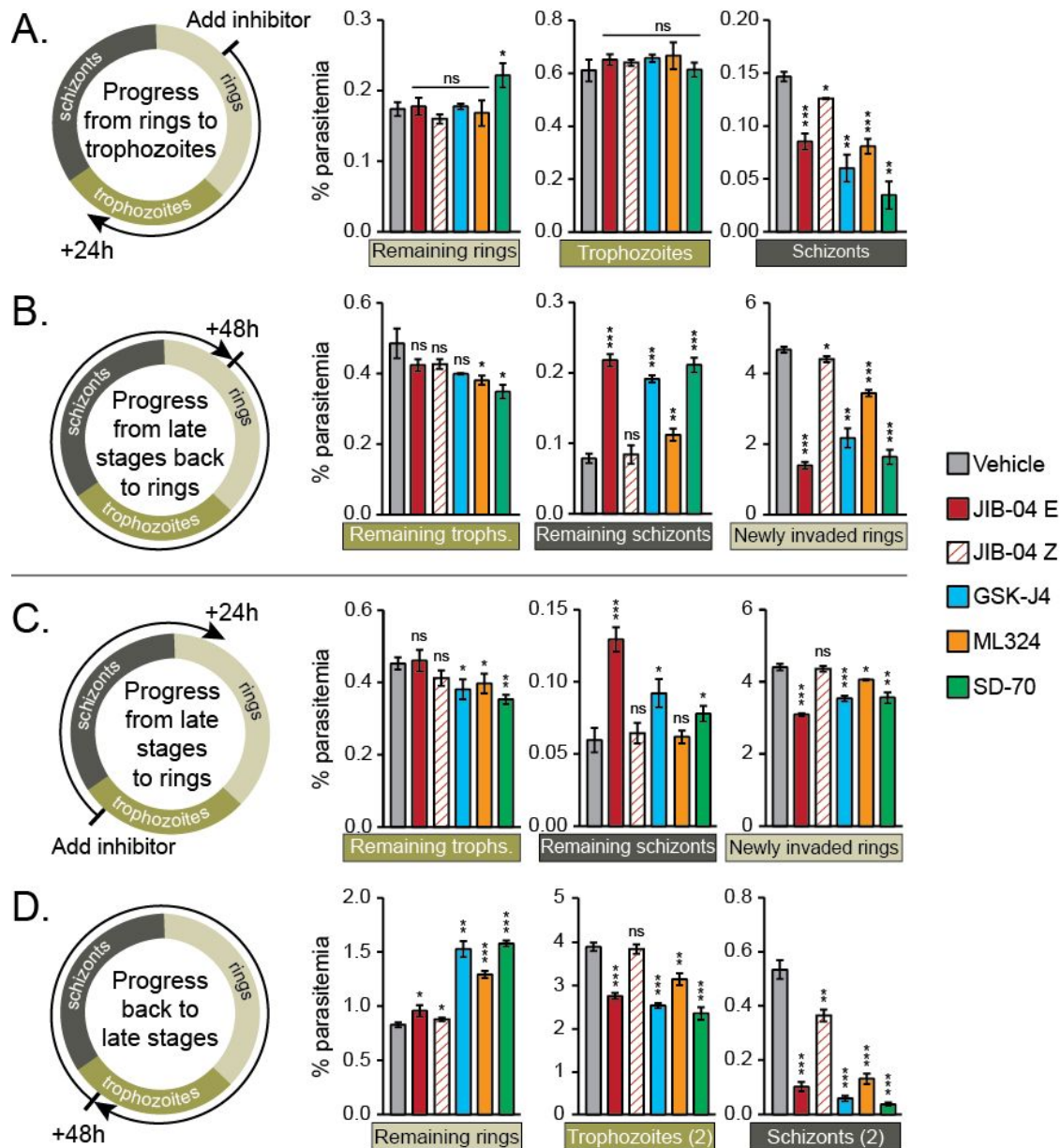


**Figure 2. Exposure of ring or late stage asexual parasites to Jumonji inhibitors significantly impairs parasite development through IDC**

Synchronized A-B) ring parasites or C-D) trophozoite parasites were grown in the presence of 1x EC50 concentrations of Jumonji inhibitors for 48 h. Quantification of parasite progression after 24 h exposure (A&C) and 48 h exposure (B&D) was monitored by flow cytometry and Giemsa stained thin blood smears as shown by representative dot plots and images in Figure S3. Ring (R), trophozoite (T), and schizont (S) parasites are gated as described in Methods. Percentages represent the average distribution of parasites within each gate as a total of infected RBCs across three technical replicates. Bar graphs present the mean  $\pm$  SD of rings, trophozoites, and schizonts as % parasitemia of triplicate wells from one of two independent experiments. P values are calculated using a t test between vehicle- and inhibitor-treated samples. n.s.: non-significant, \*  $p < 0.05$ , \*\*  $p < 0.01$ , \*\*\*  $p < 0.001$ . Scale bar = 5  $\mu$ m.

158

1  
2  
3 159 While some rings treated with JIB-04 E also progressed in the cell cycle, there were significantly  
4  
5 160 fewer parasites entering schizogony (Figure 2A, Schizonts). We observe a similar decrease in  
6  
7  
8 161 schizonts with GSK-J4, ML324, and SD-70, the other Jumonji inhibitors that showed antimalarial  
9  
10 162 activity (Figures 2A and S2A). None of these inhibitors had any effect on total parasite numbers  
11  
12 163 at this time point (Figure S2A).

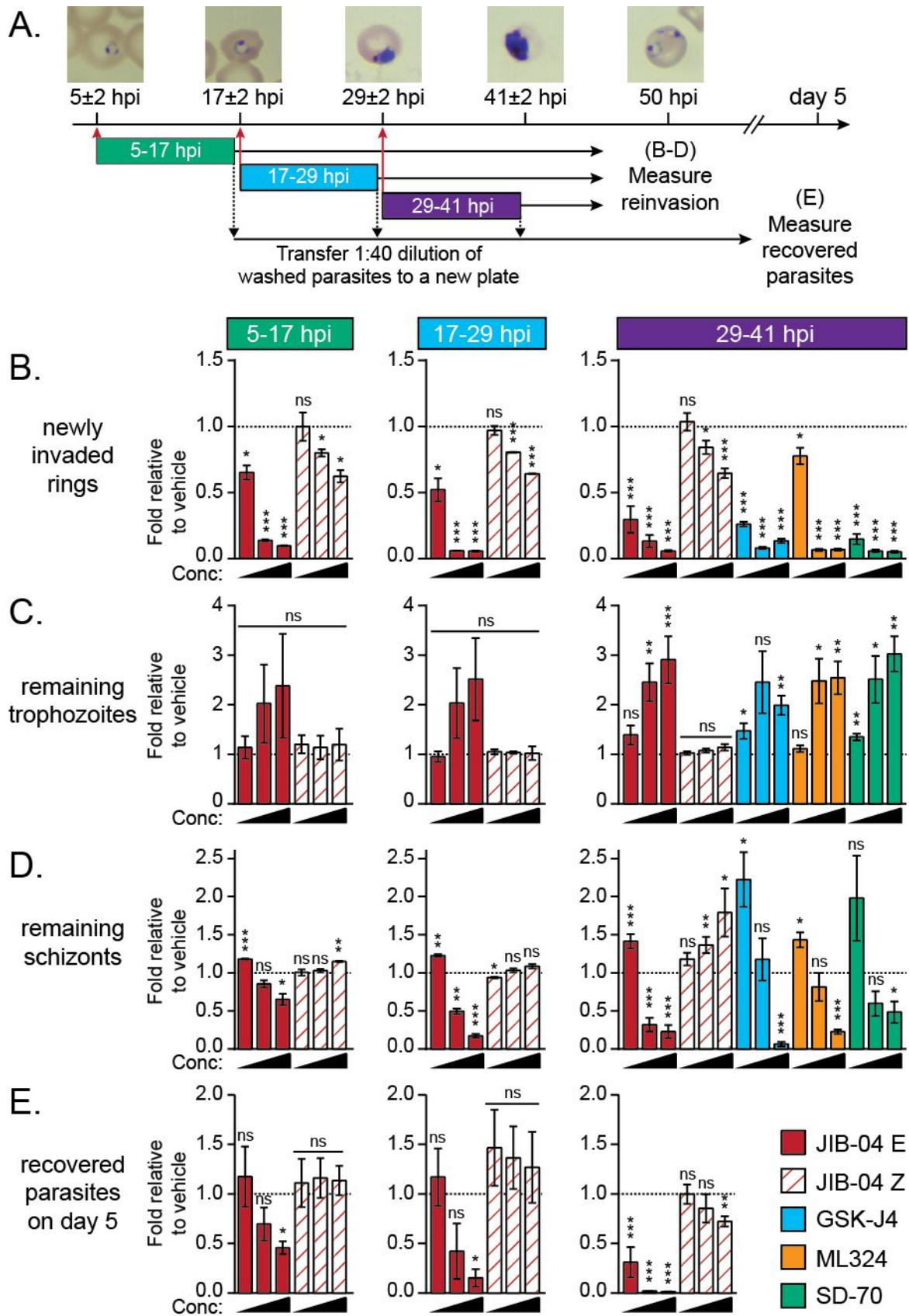
14  
15 164 After 48 h, ring parasite cultures treated with vehicle or the inactive Z isomer completed  
16  
17 165 the IDC and re-invaded new RBCs, resulting in an increase in parasitemia from ~1% to ~5%  
18  
19  
20 166 (Figure S2B). In contrast to controls, treatment with Jumonji inhibitors markedly reduced total  
21  
22 167 parasite numbers (Figure S2B). This reduction in parasitemia is mainly due to an increase in the  
23  
24  
25 168 number of remaining schizonts that have yet to complete the cell cycle, thus resulting in fewer  
26  
27 169 newly invaded rings (Figures 2B and S2B). JIB-04 E-, GSK-J4-, and SD-70-treated cultures only  
28  
29 170 had between ~1.5% - 2% newly invaded ring parasites compared to ~4.5% in controls. Treatment  
30  
31 171 with ML324 showed a more modest decrease in newly invaded rings (~3.5% rings) consistent with  
32  
33  
34 172 the higher parasitemia of these cultures.

35  
36  
37 173 To investigate if late stage parasites were susceptible to Jumonji inhibitors, we next treated  
38  
39 174 trophozoite parasites over 48 h and monitored progression through the remaining IDC and into the  
40  
41  
42 175 next cycle (Figures 2C-D and S2C-D). After 24 h, cultures treated with vehicle or the inactive  
43  
44 176 isomer Z showed enrichment in newly invaded rings and consequently increased parasitemia from  
45  
46 177 1% to ~5% (Figures 2C and S2C). Trophozoite cultures treated for 24 h with Jumonji inhibitors  
47  
48 178 showed slight decreases in the number of newly invaded rings, leading to decreased parasitemia  
49  
50  
51 179 (Figures 2C and S2C). After 48 h, the majority of parasites in control cultures progressed back to  
52  
53 180 trophozoites. In cultures treated with Jumonji inhibitors, we observed significant decreases in  
54  
55 181 trophozoites and those few parasites that have entered schizogony (Figures 2D and S2D). Parasites

1  
2  
3 182 treated with GSK-J4, ML324, SD-70, and to a lesser extent JIB-04 E, showed increased numbers  
4  
5 183 of remaining rings (Figures 2D and S2D). These results suggest that long exposure to Jumonji  
6  
7 184 inhibitors delays progression through the IDC.  
8  
9

### 10 185 *Transient exposure to Jumonji inhibitors affects all stages of the IDC*

11  
12  
13  
14 186 To test the effects of transient drug exposure throughout the IDC, we treated tightly synchronized  
15  
16 187 3D7 parasites with increasing concentrations of JIB-04 E for 12 h at defined time periods post  
17  
18 188 infection (Figure 3A). The 12 h drug exposure was carried out during ring (5–17 hpi), trophozoite  
19  
20 189 (17–29 hpi), or schizont stages (29–41 hpi). After the transient treatment, infected RBCs were  
21  
22  
23 190 washed to remove JIB-04, and re-seeded with fresh media to evaluate ability of the parasite to  
24  
25 191 proliferate post drug exposure. We then measured parasite reinvasion at ~50 hpi by flow  
26  
27 192 cytometry. About 80% of infected RBCs from vehicle-treated cultures contained newly invaded  
28  
29 193 rings constituting the bulk parasitemia, with very few trophozoites and schizonts remaining from  
30  
31 194 the previous cycle (Figure S3A). Transient exposure of rings, trophozoites, or schizonts to the  
32  
33 195 lowest concentration of JIB-04 E (1xEC<sub>50</sub>) decreased the number of newly invaded rings by 40%,  
34  
35 196 50%, and 75%, respectively, relative to vehicle-treated parasites (Figure 3B, red bars). Higher  
36  
37 197 doses (5x and 10x EC<sub>50</sub> concentrations) of JIB-04 E produce an even more severe phenotype  
38  
39 198 (Figure 3B). The decrease in newly invaded rings at 50 hpi corresponds to an increase in remaining  
40  
41 199 trophozoites that failed to complete the IDC (Figure 3C). In line with the data from Figure 2,  
42  
43 200 exposure of rings, trophozoites, or schizonts to the lowest concentration of JIB-04 E caused a  
44  
45 201 slight, but significant increase in remaining schizonts (Figure 3D). However, with increasing  
46  
47 202 concentrations of JIB-04 E, we observed an accumulation of trophozoites (Figure 3C) and fewer  
48  
49 203 schizonts (Figures 3D and S3A). Surprisingly, these parasites maintain a mitochondrial membrane  
50  
51 204 potential indicating they are still alive at the 50 hpi time point (Figure S3B). Transient exposure to  
52  
53  
54  
55  
56  
57  
58  
59  
60



205

the

13

**Figure 3. Transient exposure to JIB-04 E impairs development at all stages throughout the IDC with long-term consequences.**

A) Schematic of the experimental set up. Tightly synchronized parasites were exposed to vehicle, or 1.5  $\mu$ M, 7.5  $\mu$ M, or 15  $\mu$ M JIB-04 E (corresponding to 1x, 5x or 10x EC<sub>50</sub> from Figure 1) or inactive Z isomer during one of three 12 h periods: 5 to 17 hpi (green), 17 to 29 hpi (cyan), or 29 to 41 hpi (purple). Additional Jumonji inhibitors (GSK-J4, ML324, and SD-70) were only tested during the 29 to 41 hpi treatment period at 1x, 5x, 10x EC<sub>50</sub>. After the 12 h incubation, parasites were extensively washed to remove drug and returned to the incubator to continue growth. B-D) Progression through and completion of (reinvasion) the IDC was measured at 50 hpi by flow cytometry as described in Methods. B) Newly invaded rings, and C) remaining trophozoite and D) schizont parasites that failed to complete the IDC are presented as the fold change relative to vehicle-treated parasites. E) At the end of each treatment period, a 1:40 dilution of washed parasites was transferred into fresh RBCs and media, and cultured for two additional life cycles. Surviving parasites were measured on day 5 by flow cytometry and data are presented as the fold change relative to vehicle-treated parasites. Data represent the mean  $\pm$  SEM of 3-6 independent experiments. P values are calculated using a t test between vehicle- and inhibitor-treated samples. ns: non-significant, \* p<0.05, \*\* p<0.01, \*\*\* p<0.001.

inactive Z isomer at the same concentrations as E showed minor effects on progression consistent with its lower potency (see Figure 1A).

To determine if parasites are merely delayed in development compared to controls or actually arrested, we monitored the progression of late stage parasites (29-41 hpi time period) treated with the lowest concentration of inhibitor at 50, 53, 56, 60, and 72 hpi (Figure S3C). The numbers of remaining trophozoites and schizonts at 53, 56, and 60 hpi increased compared to 50 hpi. However, even at the latest time points, we do not observe additional newly invaded rings in the JIB-04 E-treated cultures, suggesting a block at the schizont to ring transition. By 72 hpi, this increase in remaining late stages has disappeared without a corresponding increase in newly invaded rings. Indeed these parasites having failed to complete the IDC and have died based on loss of membrane potential (Figure S3D). Again, we see no difference between the inactive Z isomer and vehicle (Figure S3C).

We next tested the effects of transient exposure of late stage parasites to the other Jumonji inhibitors (29-41 hpi only). Treatment with GSK-J4 (cyan bars) and SD-70 (green bars)

1  
2  
3 221 significantly reduced the number of parasites completing the IDC at all concentrations tested  
4  
5 222 (Figure 3B). Interestingly, treatment with the lowest concentration of ML324 (orange) had minor  
6  
7 223 effects on the number of newly invaded rings, whereas the higher concentrations showed similar  
8  
9 224 reductions in parasites numbers as the other Jumonji inhibitors. Similar to JIB-04 E, the decrease  
10  
11 225 in newly invaded rings upon exposure to the other inhibitors corresponds to an increase in the  
12  
13 226 remaining late stages. The lowest doses cause an accumulation of schizonts (Figure 3D), while the  
14  
15 227 higher doses have earlier effects resulting in trophozoite accumulation (Figure 3C). We further  
16  
17 228 analyzed the cell cycle progression of these remaining late stage parasites by a more in depth  
18  
19 229 analysis of the DNA content (Figure S3E). Increasing concentrations of Jumonji inhibitors result in  
20  
21 230 a greater number of parasites with 1N – 3N nuclei and fewer segmented schizonts with >3N nuclei  
22  
23 231 relative to vehicle controls. Together these data suggest that transient exposure of late stage  
24  
25 232 parasites to Jumonji inhibitors results in a cell cycle arrest phenotype.  
26  
27  
28  
29  
30

31 233 Finally, we sought to determine if transient 12 h JIB-04 treatment at different stages had  
32  
33 234 long-term effects on parasite proliferation and if effects were distinct depending on the stage of  
34  
35 235 parasites during treatment. For this purpose, after each treatment period, a 1:40 dilution of the  
36  
37 236 washed parasites was seeded into fresh media and RBCs, and cultures allowed to recover for 2.5  
38  
39 237 IDCs. On day 5 after seeding (scheme shown in Figure 3A), we measured total parasitemia by  
40  
41 238 flow cytometry. Exposure to 1xEC<sub>50</sub> concentrations of JIB-04 E for only 12 h had no significant  
42  
43 239 effect on the recovery of parasites treated during the ring (5–17 hpi) or trophozoite (17–29 hpi)  
44  
45 240 periods (Figure 3E, first red bar). However, parasitemia was inhibited by about 75% in cultures  
46  
47 241 exposed to the transient drug treatment during the schizont stage (29–41 hpi) at the low dose of  
48  
49 242 JIB-04 E relative to vehicle. At higher doses, transient exposure to JIB-04 E had long term effects  
50  
51 243 on all parasite cultures, regardless of the stage during treatment. Exposed rings were significantly  
52  
53  
54  
55  
56  
57  
58  
59  
60

1  
2  
3 244 less affected and schizonts were most severely affected, with parasitemia at the low end of  
4  
5 245 detection for the latter (Figure 3E, second and third red bars). As before, the inactive Z isomer had  
6  
7 246 little effect on parasite recovery. These results show that a 12 h transient exposure to Jumonji  
8  
9 247 inhibitors has both immediate and long-term effects on *P. falciparum* asexual development in  
10  
11 248 RBCs with late stage parasites having greater sensitivity.

### 15 249 ***Jumonji inhibitors block PfJmj3 catalysis***

18 250 To determine if our mammalian Jumonji inhibitors directly target the Plasmodium  
19 251 enzymes, we overexpressed and purified recombinant PfJmj3 as described in the Methods and  
20 252 Materials. As a control, we also purified a catalytically dead mutant version of PfJmj3 in which  
21 253 the iron binding residues (H166, D168, H342) were mutated to alanine (referred to as  
22 254 HDH>AAA). Both proteins were purified to homogeneity as confirmed by Coomassie staining  
23 255 (Figure 4A). Since the endogenous substrate for PfJmj3 is unknown, we measured conversion of  
24 256 the 2-OG co-substrate to succinate, the first step in Jumonji catalysis (Figure 4B). This step of the  
25 257 reaction is amenable to small molecule inhibition<sup>40</sup>. Increasing concentrations of wild type  
26 258 recombinant PfJmj3 resulted in increasing concentrations of succinate formation (Figure 4B). This  
27 259 activity is dependent on the cofactors, ascorbate and Fe(II), as well as the co-substrate, 2-OG,  
28 260 consistent with the action of the Jumonji family of enzymes (Figures 4C and S4A-B). In contrast  
29 261 to the wild type protein, neither heat inactivated PfJmj3 nor the HDH>AAA mutant showed  
30 262 activity. We next tested PfJmj3 enzymatic activity in the presence of JIB-04 and other mammalian  
31 263 Jumonji inhibitors. Increasing concentrations of active JIB-04 E, but not the inactive Z form,  
32 264 inhibited PfJmj3 activity with an IC<sub>50</sub> of 2.6 μM under the assay conditions, ie. micromolar enzyme

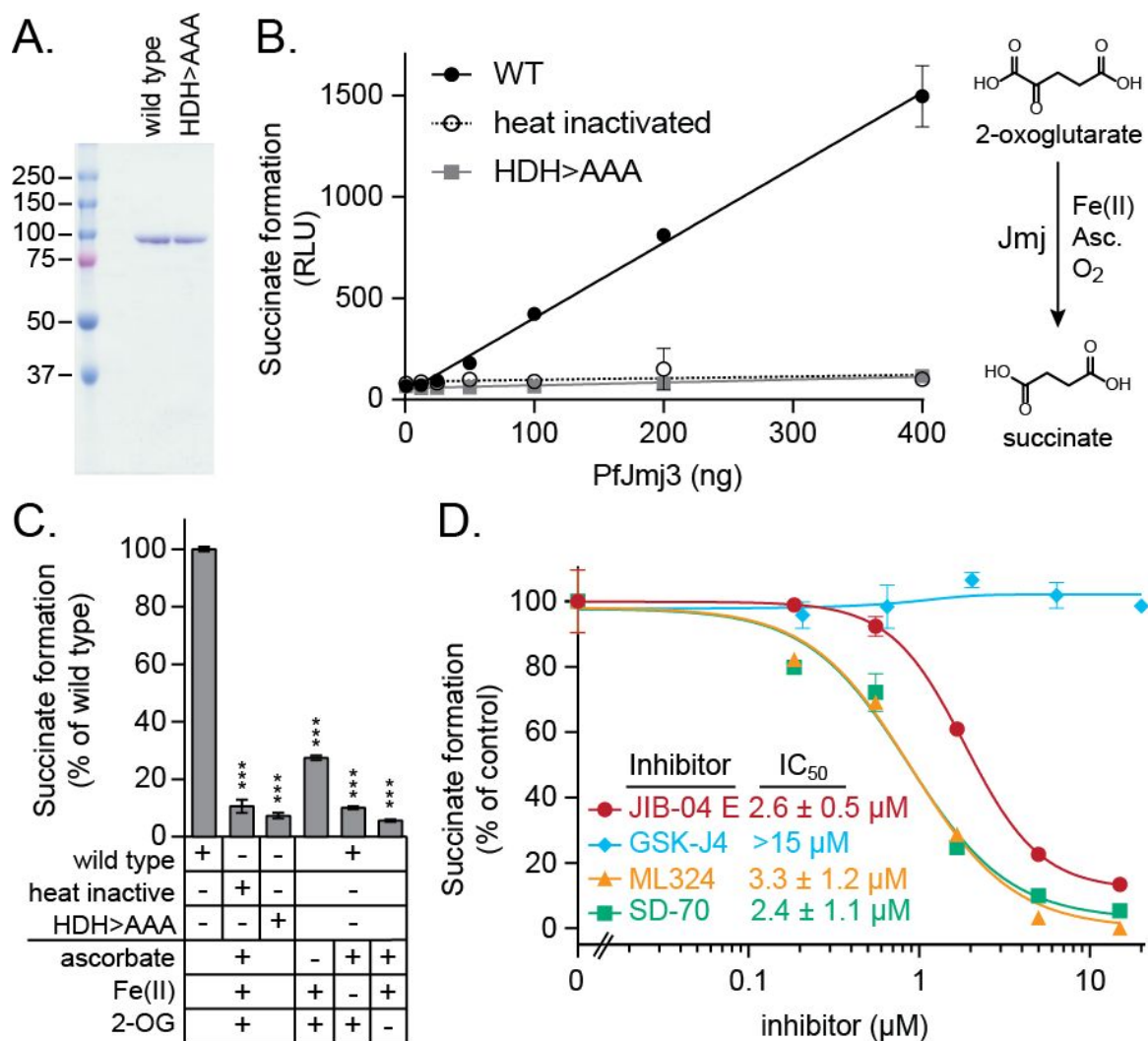


#### Figure 4. Jumonji inhibitors block the enzymatic activity of recombinant PfJmj3

A) Purity of wild type and catalytically dead (HDH>AAA) recombinant PfJmj3 as assessed by coomassie staining. B) Representative concentration curves of PfJmj3 enzymatic activity. Succinate formation is measured indirectly through a luciferase-coupled reaction (relative luciferase units (RLU)). Wild type PfJmj3, but not heat inactivated wild type or the catalytically dead HDH>AAA mutant, converts 2-OG to succinate in the presence of Fe(II), ascorbate, and O<sub>2</sub>. Data are presented as the mean ± SD of two technical replicates from 1 of 3 independent experiments. C) Succinate formation by PfJmj3 is dependent upon ascorbate, Fe(II), and 2-OG. Data are presented as a percent of wild type and represent the mean ± SEM of 3-9 independent experiments. P values are calculated using a t test between vehicle- and inhibitor-treated samples. ns: non-significant, \* p<0.05, \*\* p<0.01, \*\*\* p<0.001. D) Jumonji inhibitors block formation of succinate by PfJmj3 in a dose-dependent manner. Data are presented as a percent of the vehicle control and represent the mean ± SD of two technical replicates from 1 of 4-5 independent experiments. IC<sub>50</sub> concentrations (μM) are the mean ± SEM of the fitted inhibition curves ([Inhibitor] vs. response - Variable slope (four parameters)) from 4-5 independent experiments using GraphPad Prism v8. (Figure S4C). ML324 and SD-70 also inhibited PfJmj3 activity with similar IC<sub>50</sub> concentrations,

265  
266

1  
2  
3 267 3.3  $\mu\text{M}$  and 2.4  $\mu\text{M}$ , respectively (Figure 4D). Interestingly, GSK-J4 had no effect on PfJmj3  
4  
5 268 activity suggesting this Jumonji inhibitor does not exert its antimalarial effects through PfJmj3  
6  
7 269 inhibition. These data indicate that JIB-04, ML324, and SD-70 have the capability of directly  
8  
9 270 blocking the catalysis of 2-OG to succinate by PfJmj3, the first step in all Jumonji reactions  
10  
11 271 independent of substrate.  
12  
13  
14

### 15 272 ***JIB-04 E increases global levels of tri-methylated histones***

16  
17  
18 273 Of the two families of histone demethylases, only Jumonji proteins are enzymatically capable of  
19  
20 274 catalyzing the demethylation of tri-methylated lysine residues in histones <sup>12, 21</sup>. To investigate if  
21  
22 275 Jumonji inhibitors target histone methylation patterns in *P. falciparum* similar to their action in  
23  
24 276 mammalian cells, we performed high-resolution nanoLC-MS/MS to quantify changes in histone  
25  
26 277 post-translational modifications. Histones were purified from parasites treated acutely with 4.5  $\mu\text{M}$   
27  
28 278 JIB-04 E (3x  $\text{EC}_{50}$ ) or vehicle for 6 h starting at 29 hpi since these parasites showed higher  
29  
30 279 sensitivity (see Figure 3 in which parasites were treated with 5x and 10x  $\text{EC}_{50}$  concentrations for  
31  
32 280 12 h). Consistent with the action of Jumonji inhibitors, we observed significant increases in tri-  
33  
34 281 methylation of H3K4 (a histone mark associated with gene activation in *P. falciparum* <sup>5</sup>).  
35  
36 282 Similarly, we observed increased H3K9me3 levels (a heterochromatin mark in *P. falciparum*) and  
37  
38 283 H4K20me3 (proposed to mark active/poised chromatin) after exposure to JIB-04 E (Figure 5A) <sup>5</sup>.  
39  
40 284 <sup>41-43</sup>. There were significant decreases in the unmethylated residues for all three measured marks  
41  
42 285 and lower mono- and di-methylated forms for H4K20 (Figure 5A). Levels of tri-methyl H3K36,  
43  
44 286 the reported *var*-specific silencing mark, were below the levels of detection in both inhibitor-  
45  
46 287 treated and control samples <sup>15, 44</sup>. Together, these results suggests specific inhibition of Jumonji  
47  
48 288 tri-methyl-demethylase enzyme activities.  
49  
50  
51  
52  
53  
54  
55  
56  
57  
58  
59  
60

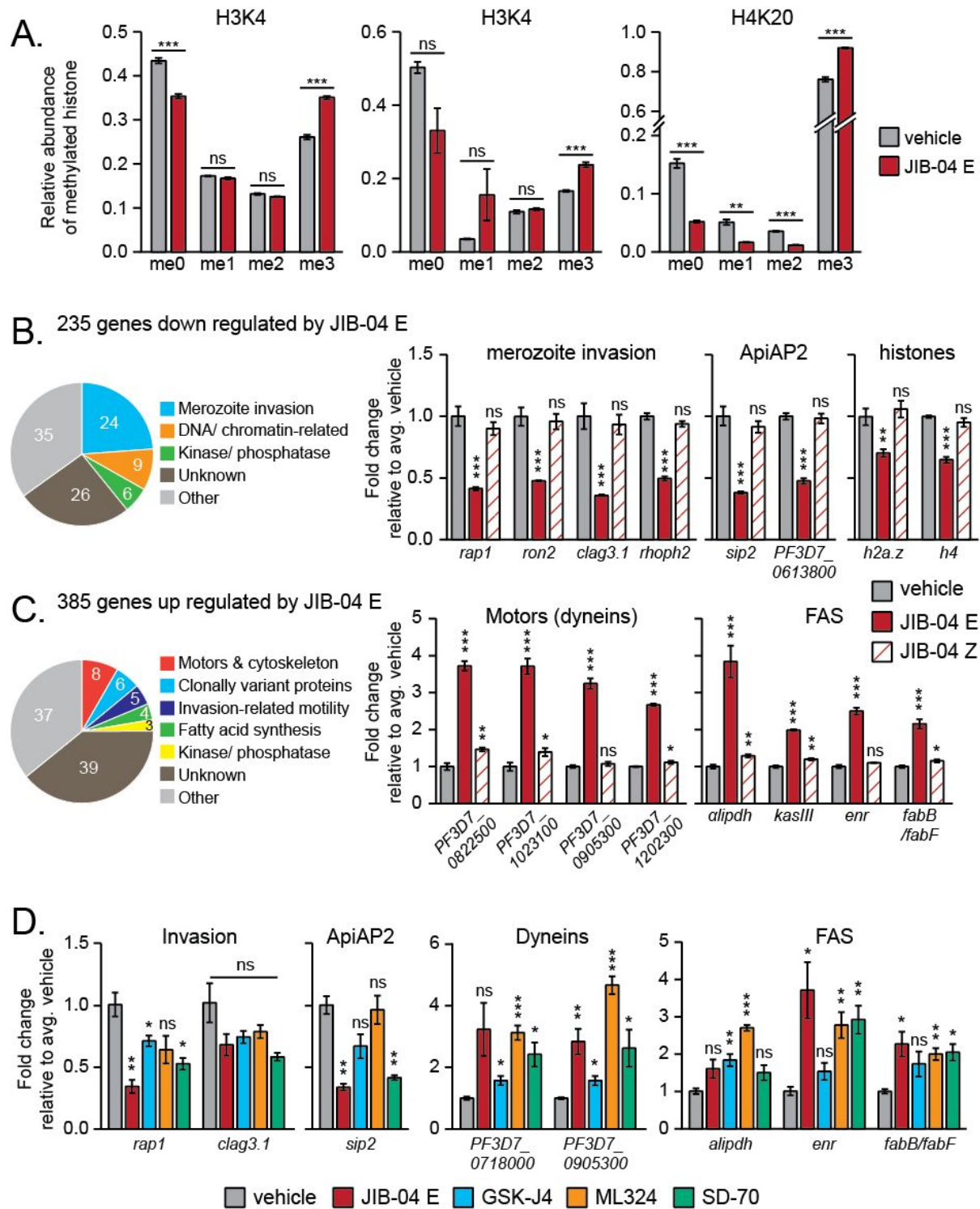


**Figure 5. JIB-04 E increases global tri-methylated histone marks and de-regulates transcription in IDC**

A) Relative abundance of histone methylation on H3K4, H3K9, and H4K20 in 29 hpi parasites treated with vehicle or 4.5  $\mu$ M JIB-04 E for 6 h. Bar graphs represent the mean  $\pm$  SEM of three biological replicates. P values are calculated using a t test between vehicle- and inhibitor-treated

289

1  
2  
3 **Figure 5 cont.** samples. B & C) Functional categorization of genes whose expression levels are  
4 deregulated by JIB-04 E based on gene ontology analysis and literature review. See also Table S3.  
5 Examples of genes B) down- or C) up-regulated in 29 hpi parasites treated for 6 h with 4.5  $\mu$ M  
6 JIB-04 E compared to vehicle and Z isomer. Data are presented as the fold change relative to  
7 vehicle-treated controls (mean  $\pm$  SEM of four replicates). P values are calculated using a t test  
8 between vehicle- and inhibitor-treated samples. D) qRT-PCR analysis of select genes from 29 hpi  
9 parasites treated with vehicle or 3x EC<sub>50</sub> concentrations of Jumonji inhibitors for 6 h as above.  
10 Data are presented as the mean  $\pm$  SEM of the fold change relative to vehicle-treated controls from  
11 three biological replicates. P values are calculated using a t test between vehicle- and inhibitor-  
12 treated samples. n.s: non-significant, \* p<0.05, \*\* p<0.01, \*\*\* p<0.001.

13  
14 290 We also examined histone methylation in parasites treated with the more selective  
15 291 mammalian Jumonji inhibitor, GSK-J4, which showed activity against asexual stage parasites in  
16  
17 292 culture (see Figure 1A), but not against recombinant PfJmj3 (see Figure 4D). GSK-J4-treated (9  
18 293  $\mu$ M, 3x EC<sub>50</sub>) parasites showed higher tri-methylation of H3K4 and H4K20 similar to JIB-04-  
19 294 treated parasites, but no changes in H3K9me3 (Figure S5A). In contrast to methylation, we  
20 295 observed no changes in the levels of acetylated histones, including the transcriptionally-coupled  
21 296 H3K9ac, H3K14ac, and H4K8ac marks in parasites treated with either Jumonji inhibitor (Figure  
22 297 S5A-B)<sup>17, 43, 45-46</sup>. These results show that exposing malaria parasites to Jumonji inhibitors disrupts  
23 298 histone tri-methylation patterns (more broadly for JIB-04 than for GSK-J4), likely causing  
24 299 deregulation of transcriptional cascades.  
25  
26  
27  
28  
29  
30  
31  
32  
33  
34  
35  
36  
37  
38

### 39 301 ***Jumonji inhibitors disrupt normal gene activation and silencing in *P. falciparum****

40  
41  
42 302 Given the changes in histone methylation observed above and the role of histone methylation in  
43 303 transcriptional regulation, we next determined the effect of Jumonji inhibitors on the *P. falciparum*  
44 304 transcriptome. We first performed global transcriptional profiling on 29 hpi 3D7 late stage  
45 305 parasites treated with either vehicle, 4.5  $\mu$ M JIB-04 E, or 4.5  $\mu$ M inactive Z isomer for just 6 h as  
46 306 above, to avoid secondary effects on parasite viability. RNA was isolated from four replicates and  
47 307 prepared for sequencing using the Illumina-based platform. We obtained expression data for over  
48 308 5,300 genes, which mapped to 94% of the *P. falciparum* genome. Unsupervised hierarchical

1  
2  
3 309 clustering segregated vehicle- and inactive Z-treated samples away from JIB-04 E-treated samples  
4  
5 310 (Figure S5C) indicating reproducible transcriptional changes. Differential expression analysis was  
6  
7 311 performed with a cut-off value of 1.5-fold change and FDR of 0.05 (Figure S5D). A comparison  
8  
9 312 of differentially expressed genes between JIB-04 E and control cultures resulted in 235 down-and  
10  
11 313 385 up- regulated genes (Figure 5B-C and Table S3), representing ~4.5% and 7.5% of the *P.*  
12  
13 314 *falciparum* genome, respectively. Unlike HDAC inhibitors, we do not see a global disruption of  
14  
15 315 the transcriptome <sup>47-48</sup>.

16  
17  
18  
19  
20 316 The majority of gene functional groups that have a defined temporal expression throughout  
21  
22 317 the IDC were not affected by JIB-04 E (Table S4 and Figure S5E) <sup>49</sup>. The one exception was  
23  
24 318 downregulation of merozoite invasion genes (Fisher exact test, probability =  $1 \times 10^{-9}$ , Figure 5B and  
25  
26 319 Table S4). This was confirmed by Gene Ontology (GO) and Malaria Parasite Metabolic Pathways  
27  
28 320 (MPMP) analysis of the 235 genes downregulated by JIB-04 E, which indicated that 24% are  
29  
30 321 related to merozoite invasion (Figure 5B and Tables S3, 'GO terms-Down' tab, and S4, 'Statistical  
31  
32 322 analysis' tab). The expression of invasion-related gene families, including *clag*, *rap*, and *ron*, are  
33  
34 323 significantly decreased by JIB-04 E, but not the inactive Z isomer (Figures 5B and S5F, and Table  
35  
36 324 S4). A similar pattern was seen with components of the glideosome (*gap* and *gapm* gene families)  
37  
38 325 (Figure S5F and Table S4).

39  
40  
41  
42  
43  
44 326 In addition to invasion genes, other gene categories identified by gene ontology  
45  
46 327 downregulated by JIB-04 included DNA/chromatin related genes (9% of the 235 genes) and  
47  
48 328 kinase/phosphatase genes (6%) (Figure 5B). For example, several histones, and histone- and DNA-  
49  
50 329 binding genes were significantly inhibited in JIB-04 E-treated parasites including AP2  
51  
52 330 transcription factors (*sip2*, *ap2-o2*, *PF3D7-0613800*, and *PF3D7\_082100*). Together, these data  
53  
54 331 indicate that JIB-04 E treatment downregulates discreet developmental pathways in *P. falciparum*.

1  
2  
3 332 In addition, JIB-04 also downregulates genes of unknown function and genes that do not fall into  
4  
5 333 major biological categories, which together represent undefined drug targets.  
6  
7

8  
9 334 The majority of the 385 genes upregulated by JIB-04 E were either of unknown function  
10  
11 335 (39%) or did not fall into functional categories (37%) as shown in Figure 5C. The remaining 24%  
12  
13 336 upregulated genes were divided among gene families related to motors and cytoskeleton, clonally  
14  
15 337 variant proteins, invasion-related motility, fatty acid synthesis, and kinases/phosphatases (Table  
16  
17 338 S3, GO terms-Up tab). For example, JIB-04 E treatment caused an increase in several dynein,  
18  
19 339 kinesin, and myosin genes (Figure 5C and Table S3). JIB-04 E also upregulated variant surface  
20  
21 340 protein genes known to be controlled epigenetically including rifins (Figure S5G and Table S3)<sup>5,</sup>  
22  
23 341<sup>15, 41</sup>. Among the upregulated fatty acid synthesis genes were *fab b/f*, *kasIII*, and *enr* and genes  
24  
25 342 encoding enzymes acting on pyruvate upstream of acetyl CoA production (Figure 5C and Table  
26  
27 343 S3).  
28  
29  
30  
31

32  
33 344 To validate the generality of the above transcriptional changes induced JIB-04 E, we  
34  
35 345 performed qRT-PCR on a subset of genes deregulated by JIB-04 E on parasites treated with the  
36  
37 346 other Jumonji inhibitors (Figures 5D and S5H-I). In agreement with the RNAseq data, GSK-J4,  
38  
39 347 ML324, and SD-70 showed a similar trend to JIB-04 E in reducing the expression of *rap1*, *clag3.1*  
40  
41 348 (Figure 5D), *ron2*, and *gap50* (Figure S5H) from the various invasion-related gene families.  
42  
43 349 Various Jumonji inhibitors also downregulated expression of DNA/chromatin-related genes such  
44  
45 350 as the AP2 transcription factor *sip2* (Figure 5D) and histones (Figure S5H). Similar to JIB-04 E,  
46  
47 351 several Jumonji inhibitors activated expression of genes involved in motor activity and invasion  
48  
49 352 (dynein heavy chains, *ctrp*, *tramp*, and *plasmepsin X*) and fatty acid synthesis (*alipdh*, *enr*, and *fab*  
50  
51 353 *b/f*) (Figures 5D and S5I). Interestingly, we observed weaker activation of some genes by GSK-J4  
52  
53  
54  
55 354 compared to the other Jumonji inhibitors. Thus regulation of these gene sets generally parallel the  
56  
57  
58  
59  
60

1  
2  
3 355 antimalarial activity of the inhibitors, their effects on parasite progression through the IDC, their  
4  
5 356 effects on histone tri-methylation, and their inhibition of PfJmj3 activity *in vitro*.

7  
8  
9 357 ***JIB-04 E modulated genes are targets of specific transcriptional regulators***

10  
11 358 Regulation of invasion genes during the IDC is mediated in part through binding of the AP2  
12  
13 359 transcription factor AP2-I to the “rhostry motif,” found upstream of invasion-related genes  
14  
15 360 including *rap* and *rhoph* gene families<sup>19, 50</sup>. PfAP2-I activates transcription of genes in concert  
16  
17 361 with two associated chromatin reader proteins, bromodomain protein 1 (PfBDP1) and  
18  
19 362 chromodomain protein 1 (PfCHD1)<sup>50</sup>. BDP1, which binds H3K9ac *in vitro*, was also found  
20  
21 363 enriched upstream of micronemal genes likely regulating these genes in complex with another AP2  
22  
23 364 transcription factor<sup>50-51</sup>. We find that 36% of genes bound by PfAP2-I (Fisher t-test,  $p = 2.2 \times$   
24  
25 365  $10^{-6}$ ) and 22% of PfBDP1 target genes (Fisher t-test,  $p = 1.7 \times 10^{-13}$ ) are downregulated by JIB-04  
26  
27 366 E (Figure 6A and Table S3, ‘RNAseq\_Down’ tab)<sup>50-51</sup>. Of the 89 genes that are co-regulated by  
28  
29 367 both PfAP2-I and PfBDP1, JIB-04 E inhibits 54 of them (ie, 60% of genes in this entire set)  
30  
31 368 including invasion-related gene families (*rap*, *rhoph*, *gap*, *gapm*) and several kinases, two of which  
32  
33 369 (PKAr and PKAc) are involved in parasite egress<sup>52-53</sup>. PfBDP1 and PfAP2-I also co-bind the  
34  
35 370 promoters of a number of nucleosome and chromatin-binding genes including histones and seven  
36  
37 371 AP2 genes<sup>50</sup>. Of these, JIB-04 E down regulates 3 core histones, 2 variant histones, *set10*, *chd1*,  
38  
39 372 and the AP2 transcription factor, *sip2* (Table S3). An additional 63 genes targeted by PfBDP1, but  
40  
41 373 not PfAP2-I, were also downregulated by JIB-04 E (Figure S6A). These include additional rhostry  
42  
43 374 genes (*ron*, *msp*) as well as an AP2 transcription factor (*PF3D7\_0613800*). Furthermore, an  
44  
45 375 additional 20 genes bound by PfAP2-I, but not PfBDP1, were also significantly affected by JIB-  
46  
47 376 04 E treatment (Table S3). These results suggest that JIB-04 E prevents activation of invasion-  
48  
49 377 related genes as

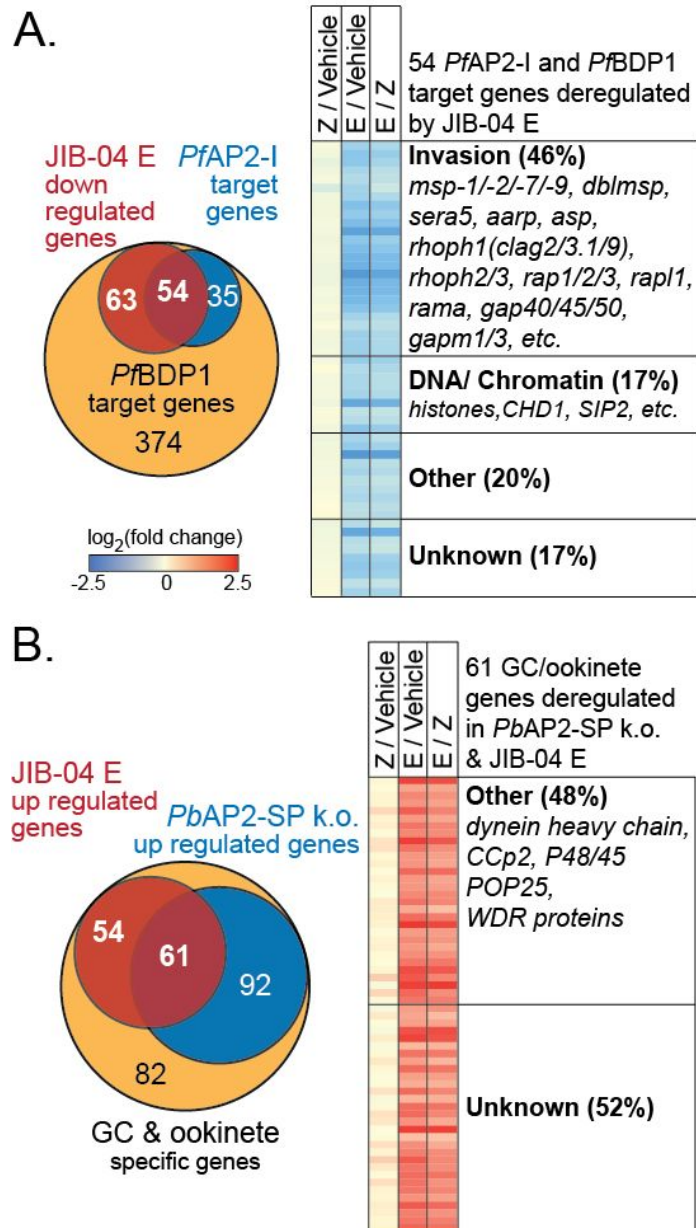


**Figure 6. JIB-04 E deregulates genes that overlap known invasion and gametocyte transcription- and chromatin-binding factor targets**

A) Venn diagrams of genes downregulated by JIB-04 E (red) that overlap with PfBDP-1 (orange) and PfAP2-I (blue) target genes. Heat map showing the differential expression between JIB-04 E and controls of the 54 genes common to all three groups. See also Table S3. B) Venn diagrams showing the overlap of genes upregulated by JIB-04 E (red) with gametocyte and ookinete-specific genes (orange) and genes upregulated in *P. berghei* schizonts lacking PbAP2-SP (blue). Heat map showing the differential expression between JIB-04 E and controls of the 61 genes common to all three groups. See also Tables S3-4.

378 well as DNA- and chromatin-binding genes by interfering, either directly or indirectly, with  
 379 transcriptional activating complexes containing PfBDP1 and/or PfAP2-I. Indeed, JIB-04 E  
 380 treatment strongly mimics the transcriptional changes observed in the BDP1 knockdown and  
 381 downregulates 34 out of the 47 genes decreased upon BDP1 loss of function ( $p = 2.2 \times 10^{-16}$ ; Table  
 382 S3)<sup>51</sup>.

1  
2  
3 384 We noted that many of the genes upregulated by JIB and not expressed in our control  
4  
5 385 parasites (<5 RPKM) have predicted roles in the other stages of the *P. falciparum* life cycle. Using  
6  
7  
8 386 a manually curated data set from a literature search, we analyzed this gene set against genes known  
9  
10 387 to be specifically expressed in gametocyte and ookinete stages (Tables S3, ‘RNAseq\_Up’ tab, and  
11  
12 388 S4, ‘GC-ookinete list’ tab)<sup>18, 54</sup>. We find that 115 of the 385 genes upregulated by JIB-04 E are  
13  
14 389 expressed >5-fold higher in gametocytes or ookinetes compared to asexual parasites (Fisher t-test,  
15  
16 390  $p = 2.2 \times 10^{-16}$ ) (Figure 6B and Tables S3-4). These sexual-stage genes are expressed at relatively  
17  
18 391 low levels in the control cultures (<5 RPKM) and JIB-04 E treatment activates them (Figures 6B  
19  
20 392 and S6B). We also found significant overlap (162 of 385) with genes upregulated in the knockout  
21  
22 393 of PbAP2-SP (Fisher t-test,  $p = 2.2 \times 10^{-16}$ ), a transcription factor essential for the development of  
23  
24 394 infectious ookinetes in *P. berghei* (Tables S3-4)<sup>55</sup>. 61 of these genes were also highly expressed  
25  
26 395 in sexual stages and overlap among the three data sets (Figure 6B). These include gametocyte-  
27  
28 396 specific genes, such as 6-cysteine protein P48/45 and several WD40 repeat (WDR) proteins, as  
29  
30 397 well as ookinete-specific genes, such as PSOP25 (Figure S6B). Parasites treated with the other  
31  
32 398 Jumonji inhibitors also show abnormal activation of the gametocyte-specific gene, *pf11-1*, and the  
33  
34 399 ookinete-specific AP transcription factor, *ap2-o3* (Figure S6C). These results suggest that JIB-04  
35  
36 400 E is activating genes normally silenced during the *P. falciparum* IDC possibly through a  
37  
38 401 transcription factor functionally akin to *P. berghei*’s AP2-SP. Overall, Jumonji inhibitors thus  
39  
40 402 disrupt only discreet programs of the normal *P. falciparum* transcriptome including blocking  
41  
42 403 invasion related gene-activation and aberrantly turning on the expression of genes specific to  
43  
44 404 sexual parasite forms, without globally altering gene expression patterns.  
45  
46  
47  
48  
49  
50  
51  
52  
53  
54  
55  
56  
57  
58  
59  
60

## 405 Discussion

406 In this study, we took a pharmacological and biochemical approach to probe the role of  
407 Jumonji enzymes in the malaria parasite, *Plasmodium falciparum*. We show that several small  
408 molecule inhibitors of mammalian Jumonji histone lysine demethylases disrupt growth of asexual  
409 and sexual stage parasites. In fact, gametocyte development and the formation of gametes are  
410 highly sensitive to JIB-04 E with EC<sub>50</sub> concentrations in the nanomolar range (0.01 – 0.12 μM).  
411 This hypersensitivity towards sexual stages compared to asexual stages could result from  
412 differences in the expression levels and/or essentiality of the PfJmj enzymes during  
413 gametocytogenesis and gamete formation leading to transcriptional disruption of gene programs  
414 involved in sexual development. Alternatively, variations in iron, 2-OG, oxygen, ascorbic acid,  
415 and even succinate levels between the stages could contribute to this difference in potency.  
416 Previous studies have demonstrated that inhibitors of histone lysine methyltransferases (KMTs),  
417 the writers of methylation, block asexual stage growth, gametocyte development, and gamete  
418 formation<sup>56-58</sup>. Male gametes were about 10-fold more susceptible to inhibition of the G9a KMT  
419 than female gametes<sup>57</sup>. We observe a similar shift in EC<sub>50</sub> with the Jumonji inhibitor JIB-04 E  
420 (0.01 vs 0.08 μM for male vs female gamete formation), highlighting an essential role of histone  
421 methylation homeostasis for transmission to the anopheline vector.

422 Studies targeting histone acetyl transferase, histone deacetylase, and KMT enzymes have  
423 implicated histone modifications in regulating the complex life cycle of the malaria parasite, but  
424 the role of KDMs, the erasers of methylation, remained largely unstudied<sup>47-48, 56-63</sup>. Jiang *et al.*  
425 have shown that neither PfJmjC1 nor PfJmjC2 is essential for *in vitro* asexual development in the  
426 erythrocyte<sup>15</sup>. Interestingly, neither the *PfJmjC1* nor *PfJmjC2* knockout mimicked the *var* gene  
427 deregulation phenotype of the *SETvs* KMT knockout suggesting redundancy or compensation of

1  
2  
3 428 KDM activity by another PfJmj enzyme<sup>15</sup>. In a recent transposon mutagenesis screen, PfJmj3  
4  
5 429 mutant parasites while viable did exhibit a low mutagenesis fitness score (-2.57) indicating a  
6  
7 430 fitness cost for *in vitro* asexual growth due to disruption of the gene<sup>20</sup>. Unlike the above studies,  
8  
9  
10 431 our approach using small molecule inhibitors potentially targets all three *P. falciparum* Jumonji  
11  
12 432 enzymes. Our *in vitro* biochemical studies show that Jumonji inhibitors inhibit the enzymatic  
13  
14 433 activity of recombinant PfJmj3, while our molecular and mass spectrometry data suggest that  
15  
16 434 inhibitors reduce Jumonji histone demethylase activity on multiple tri-methylated histone marks.  
17  
18  
19 435 Thus their action on the parasite is at least partly on target and may represent the cumulative effect  
20  
21 436 on multiple Jumonji enzymes. Of interest is the difference between GSK-J4 and the other inhibitors  
22  
23 437 evaluated here. GSK-J4 does not inhibit the enzymatic activity of PfJmj3 *in vitro* nor does it  
24  
25 438 increase the levels of H3K9me3 in the parasite, in contrast with JIB-04. It does, however, increase  
26  
27 439 other tri-methyl histone marks including H3K4me3 and H4K20me3, suggesting a different target  
28  
29 440 specificity from JIB-04, ML324, and SD-70.  
30  
31  
32  
33

34 441 Tri-methylation of multiple lysine residues on H3 and H4 has been well documented in *P.*  
35  
36 442 *falciparum*. H3K4me3 is a euchromatic mark highly enriched in late stage asexual parasite<sup>5, 17, 45,</sup>  
37  
38 443 <sup>64-66</sup>. Although the exact role of this mark in *P. falciparum* is still unclear, it is likely associated  
39  
40 444 with transcriptional activity<sup>67</sup>. H3K9me3 is a repressive mark specifically localized to telomeres  
41  
42 445 and subtelomeric repeats and has a well characterized role in regulating clonally variant gene  
43  
44 446 expression in *P. falciparum*<sup>5, 11, 42, 68</sup>. The H4K20me3 mark has been reported in *P. falciparum*  
45  
46 447 with global levels peaking in schizonts, but its function in the parasite is still unknown<sup>5, 43, 45, 66</sup>.  
47  
48 448 Our studies provide evidence that mammalian Jumonji inhibitors block the histone demethylase  
49  
50 449 activity of at least one of the three *P. falciparum* Jumonji enzymes *in vivo* resulting in increased  
51  
52 450 levels of histone methylation, and/or directly block PfJmj3 catalysis *in vitro*. Given the specificity  
53  
54  
55  
56  
57  
58  
59  
60

1  
2  
3 451 achieved among the mammalian Jumonji KDMs within the active site pocket, it is plausible that  
4  
5 452 inhibitors specific to the *P. falciparum* Jumonji's might be designed without toxicity to healthy  
6  
7 453 cells. Furthermore, since in the cancer setting JIB-04 and other inhibitors have shown robust  
8  
9 454 selectivity for the disease state, not affecting normal cells, there is potential for parasite-targeting  
10  
11 455 analogs to have a strong therapeutic window against the most sensitive sexual stages.  
12  
13  
14

15 456 In line with the disruption of tri-methyl histone marks, JIB-04 E altered expression of 620  
16  
17 457 genes in parasites (~12% of the *P. falciparum* genome). We observed up- and down-regulation of  
18  
19 458 gene expression leading to misregulation of specific transcriptional programs, in agreement with  
20  
21 459 the discreet effects of Jumonji inhibitors also seen in cancer cells and tumors <sup>32, 69</sup>. These  
22  
23 460 transcriptional changes were replicated with other Jumonji inhibitors, indicating overlapping  
24  
25 461 mechanism of action and common gene targets. Our results are in contrast to the effects of HDAC  
26  
27 462 inhibitors such as apicidin and trichostatin A, which caused more global changes of the IDC  
28  
29 463 transcriptome affecting from ~30% up to 60% of the *P. falciparum* genome <sup>47-48</sup>.  
30  
31  
32  
33

34 464 The majority of genes downregulated by Jumonji inhibition were either annotated as  
35  
36 465 unknown function or did not fall into any known GO group, representing yet undefined targets of  
37  
38 466 Jumonji inhibition. Of interest, a subset of downregulated genes were enriched in invasion-related  
39  
40 467 genes and a surprising number coincided with loci regulated in *P. falciparum* by the chromatin  
41  
42 468 reader PfBDP1, the PfAP2-I transcription factor, or both. PfBDP1 and PfAP2-I have been directly  
43  
44 469 implicated as master regulators of invasion gene programs in recent genetic studies <sup>50-51</sup>.  
45  
46 470 Conditional PfBDP1 knockdown blocks parasite invasion and growth <sup>51</sup>. PfBDP1 has not yet been  
47  
48 471 pharmacologically targeted, and targeting transcription factors such as PfAP2-I is notoriously  
49  
50 472 challenging. Jumonji inhibitors partly disrupt PfBDP1 and/or PfAP2-I transcriptional programs  
51  
52 473 and may thus block parasite invasive capacity through modulation of histone methylation at these  
53  
54  
55  
56  
57  
58  
59  
60

1  
2  
3 474 loci. Indeed, JIB-04 treatment mimics gene downregulation in the PfBDP1 knockdown and may  
4  
5 475 thus be a surrogate inhibitor for this chromatin interacting protein <sup>51</sup>.  
6  
7

8  
9 476 Whether the Jumonji inhibitors evaluated here are exerting their antimalarial effects also  
10  
11 477 by affecting non-transcriptional pathways remains an open question. A growing number of non-  
12  
13 478 histone targets of Jumonji enzymes, including transcription factors, enzymes and tRNA have been  
14  
15 479 identified in other systems <sup>70</sup>. This may be the case also in *Plasmodium falciparum*. It is feasible  
16  
17 480 that inhibition of PfJmjC2, for example, may affect the parasite's wybutasine pathway, disrupting  
18  
19 481 translational control since PfJmjC2 closely resembles the mammalian Jumonji enzyme TYW5 <sup>71</sup>.  
20  
21 482 Based on sequence homology, PfJmj3 aligns with Jumonji protein hydroxylases, suggesting a  
22  
23 483 potential role for protein hydroxylation in the malaria parasite in addition to histone demethylation.  
24  
25 484 Recent studies have shown that Jumonji hydroxylases have roles in protein translation, cell  
26  
27 485 division, and development <sup>72-74</sup>. For example, human JMJD7 was reported to hydroxylate lysine  
28  
29 486 residues on developmentally regulated GTP-binding proteins 1 and 2 (DRG1/2), increasing the  
30  
31 487 complex's affinity for RNA, whereas human JMJD5 can modify arginine residues on the  
32  
33 488 chromosome condensation domain containing protein 1 (RCCD1) and ribosomal protein S6  
34  
35 489 (RPS6) <sup>72-73</sup>. Thus future work will need to identify the histone, non-histone protein and non-  
36  
37 490 protein substrate(s) of all three *P. falciparum* Jumonji enzymes and establish their functional  
38  
39 491 significance. <sup>40</sup> At present, our studies provide direct evidence that mammalian Jumonji inhibitors  
40  
41 492 block malaria Jumonji enzyme activity *in vitro*, increase histone tri-methylation in the parasite,  
42  
43 493 alter discreet transcriptional programs, and disrupt parasite development. These findings suggest  
44  
45 494 that the aggregate activities of the *P. falciparum* Jumonji enzymes is likely essential during the  
46  
47 495 parasite's life cycle.  
48  
49  
50  
51  
52  
53  
54  
55  
56  
57  
58  
59  
60

1  
2  
3 496 **Conclusion**  
4

5 497 Here, we use a pharmacological and biochemical approach to probe the role of Jumonji  
6  
7 498 enzymes in the malaria parasite. Jumonji enzymes are transcriptional regulators that in other  
8  
9  
10 499 known systems erase methylation from histones affecting gene expression. We show that in  
11  
12 500 *Plasmodium falciparum* inhibitors of mammalian Jumonji enzymes trigger the accumulation of  
13  
14 501 histone methylation, deregulate gene expression programs, halt parasite development and lead to  
15  
16 502 parasite death. In vitro, the inhibitors block the catalytic activity of a purified malaria Jumonji  
17  
18 503 enzyme. Together, these findings suggest that the aggregate activity of the malaria Jumonji  
19  
20  
21 504 enzymes is likely essential during the parasite's life cycle.  
22  
23  
24  
25  
26  
27  
28  
29  
30  
31  
32  
33  
34  
35  
36  
37  
38  
39  
40  
41  
42  
43  
44  
45  
46  
47  
48  
49  
50  
51  
52  
53  
54  
55  
56  
57  
58  
59  
60

## 505 **Materials and Methods**

### 506 *Parasites and culturing*

507 For asexual stage experiments, 3D7 and Dd2 parasites were cultured at 2% to 4% hematocrit in  
508 male O<sup>+</sup> red blood cells (Valley Biomedical, Winchester, VA) in RPMI 1640 media with L-  
509 glutamine and 25 mM HEPES (Sigma-Aldrich, St. Louis, MO) supplemented with 5% Albumax  
510 I (Gibco, Life Technologies, Carlsbad, CA), 12 μg/ml hypoxanthine (Sigma, St. Louis, MO), and  
511 23 mM sodium bicarbonate <sup>75</sup>. Cultures were maintained in a humidified incubator at 37°C under  
512 a 5% O<sub>2</sub>/5% CO<sub>2</sub>/90% N<sub>2</sub> gas mixture. When parasites were maintained at a parasitemia greater  
513 than 4% for particular experiments, cultures were fed twice daily. Parasite lines were regularly  
514 tested for mycoplasma by PCR using the primers Myco Forward 5'-  
515 CCGCGGTAATACATAGGTCGC and Myco Reverse 5'-CACCATCTGTCACTCTGTAAACC.  
516 Parasitemia was monitored by blood smears stained with Giemsa (Sigma-Aldrich) diluted in pH  
517 7.2 buffer (Millipore, Billerica, MA). Images of stained parasites were acquired using an Infinity  
518 1-2CB camera and Analysis software (Lumenera Corp., Ottawa, Canada). 3D7 and Dd2 parasites  
519 were a gift from Dr. Margaret Phillips (UT Southwestern).

520 Gametocyte commitment and development assays were performed using the NF54 peg4-  
521 tdTomato reporter line <sup>76</sup> with media supplemented with 0.25% AlbuMax II (ThermoFisher,  
522 Waltham, MA) and 5% human serum (NY Blood Center, New York, NY). For the dual gamete-  
523 formation assays, NF54 parasites (MRA-1000, BEI Resources, Manassas, VA) were cultured in  
524 media supplemented with 10% human serum (obtained from Biobancos de Castilla y Leon,  
525 Barcelona and Centro de Transfusiones de Madrid and the Red Cross Transfusion Blood Bank in  
526 Madrid, Spain).

1  
2  
3 527 *Chemical compounds*  
4  
5

6 528 Chloroquine (Sigma-Aldrich) was dissolved in H<sub>2</sub>O, whereas all other drugs were dissolved in  
7  
8 529 DMSO (Sigma-Aldrich). The Jumonji inhibitors used in this study were obtained from Cayman  
9  
10 530 Chemical, Ann Arbor, MI (GSK-J4, GSK-J5, and CPI-455), Selleck Chemicals, Houston, TX  
11  
12 531 (ML324), and Xcess Biosciences, San Deigo, CA (KDM5-C70 and SD-70). JIB-04 E and Z  
13  
14 532 isomers were synthesized as previously described<sup>23</sup>. Compounds freshly dissolved in DMSO were  
15  
16 533 aliquoted to minimize freeze/thaw cycles and stored at -20°C.  
17  
18  
19  
20

21 534 *EC<sub>50</sub> determination*  
22  
23

24 535 Compound EC<sub>50</sub> concentrations were determined using the 3-day SYBR green assay as described  
25  
26 536 in Smilkstein et al with slight modifications<sup>30</sup>. Parasites were synchronized to ring stages using  
27  
28 537 5% sorbitol for two cycles prior to the experiment. On day 0, ring stage parasites were seeded into  
29  
30 538 the inner wells of a 96 well black plate with clear bottom (Costar, Tewksbury, MA) at 0.5%  
31  
32 539 parasitemia and 2% hematocrit. Drug was added such that each well received the same  
33  
34 540 concentration of DMSO (final DMSO concentration < 0.5%). Each plate contained vehicle-only  
35  
36 541 and chloroquine (0.25 μM for 3D7 and 5 μM for Dd2) controls. Parasites were incubated at 37°C  
37  
38 542 in the presence of compounds for 72 h after which thin blood smears were made and plates were  
39  
40 543 frozen at -80 °C. On a subsequent day, plates were thawed at RT and 100 μL of 2x SYBR Green I  
41  
42 544 (Sigma-Aldrich) in lysis buffer (20 mM Tris-HCl, pH 7.5, 5 mM EDTA, 0.008% w/v saponin, and  
43  
44 545 0.03% v/v Triton X-100) was added to each plate. Plates were then incubated in the dark at RT for  
45  
46 546 4 h. Fluorescence was measured on a BioTek (Winooski, VT) Synergy H1 Hybrid plate reader  
47  
48 547 using a 485nm excitation filter and a 535nm emission filter. EC<sub>50</sub> values were calculated as a  
49  
50 548 percentage of parasite viability relative to vehicle-only and chloroquine-killed controls. A non-  
51  
52  
53  
54  
55  
56  
57  
58  
59  
60

1  
2  
3 549 linear regression curve ([Inhibitor] vs. response - Variable slope (four parameters):  $Y = \text{Bottom} +$   
4  
5 550  $(\text{Top} - \text{Bottom}) / (1 + (\text{IC}_{50}/X)^{\text{HillSlope}})$  was fit to the data using GraphPad Prism version 8. Each  
6  
7  
8 551 plate contained three technical replicates. Mean  $\text{EC}_{50}$  concentrations and SEM were calculated  
9  
10 552 from at least 3 independent experiments.

### 13 553 *Gametocyte development assays*

16 554 Synchronous gametocytes were obtained following a method adapted from Fivelman *et al.*<sup>77</sup>. *P.*  
17  
18 555 *falciparum* sexual development assays were performed using the NF54 peg4-tdTomato reporter  
19  
20  
21 556 line in 96-well flat bottom plates. Twice synchronized trophozoites were cultured in suspension at  
22  
23 557 2% parasitemia and 3% hematocrit in flasks. Parasites were allowed to reinvade new red blood  
24  
25 558 cells, and the culture was maintained in the subsequent 48 h cycle at about 8-9% parasitemia and  
26  
27 559 3% hematocrit (sexual commitment cycle). At the end of the commitment cycle, segmented  
28  
29 560 schizonts were purified using a Percoll-sorbitol gradient and then combined with fresh erythrocytes  
30  
31 561 in complete media at 3% hematocrit and around 10% parasitemia for 3-4 h to allow for reinvasion.  
32  
33 562 When the ring parasitemia reached 3.5%, remaining late stages were removed via Percoll-sorbitol  
34  
35 563 gradient, and the newly invaded ring parasites were washed three times with incomplete media.  
36  
37 564 On Day +1 (first day of gametocyte development), parasitemia and pre-existing gametocytemia  
38  
39 565 were assessed by flow cytometry (Cytek DxP11) based on Hoechst 33342 DNA-staining (375nm  
40  
41 566 laser, 450/50 emission filter) and the tdTomato fluorescent signal (561nm laser, 590/20 emission  
42  
43 567 filter). Plates were set up with 200  $\mu\text{L}$  drug-media per well containing the compound of interest  
44  
45 568 and 50 mM N-acetylglucosamine at 3.5% parasitemia and 1% hematocrit. Parasites were cultured  
46  
47 569 for an additional six days to allow for gametocyte development, during which media was not  
48  
49 570 changed. On Day +6, the gametocytemia was assessed by flow cytometry using Hoechst 33342  
50  
51 571 DNA-staining and tdTomato fluorescent signal.

1  
2  
3 572 *Gamete formation assays*  
4  
5

6 573 The dual gamete-formation assay was performed as described in Delves *et al*<sup>37</sup>. NF54 parasites  
7  
8 574 were cultured in media supplemented with 10% human serum and induced to form gametocytes.  
9  
10 575 On day 14 post induction, stage V gametocytes were seeded into 384-well plates at 1%  
11  
12 576 gametocytemia and 4% hematocrit and exposed to drug for 48 h. To induce male exflagellation  
13  
14 577 and monitor female gametes, ookinete media containing 100  $\mu$ M xanthurenic acid (Sigma-Aldrich)  
15  
16 578 and 0.5  $\mu$ g/mL anti-Pfs25-cy3 antibody (MRA-315, BEI Resources) was added. Exflagellation  
17  
18 579 was monitored by phase contrast on a Nikon Ti-E widefield microscope. Plates were incubated for  
19  
20 580 an additional 24 h and female gamete formation was evaluated by the expression of Pfs25 on the  
21  
22 581 TRITC channel. Exflagellation centers and female gamete formation were quantified using the Icy  
23  
24 582 Bioimage Analysis Program (<http://icy.bioimageanalysis.org/>). Inhibition of gamete formation by  
25  
26 583 JIB-04 was calculated relative to positive (40  $\mu$ M gentian violet, MolPort) and negative (DMSO)  
27  
28 584 controls.  
29  
30  
31  
32  
33

34  
35 585 *Flow cytometry*  
36  
37

38 586 Live infected red blood cells were labeled for 30 minutes in the dark with final concentrations of  
39  
40 587 dyes at 4  $\mu$ M Hoechst 33342 (Molecular Probes, Eugene, OR), 100 ng/mL thiazole orange (Sigma-  
41  
42 588 Aldrich), and 25 nM DiIC<sub>1</sub>(5) (1,1',3,3',3',3'-Hexamethylindodicarbocyanine Iodide, Molecular  
43  
44 589 Probes). Progression through the asexual IDC was assessed by flow cytometry (5-laser BD FACS  
45  
46 590 Aria Fusion SORP or FACS Aria Fusion; The Moody Foundation Flow Cytometry Facility, UT  
47  
48 591 Southwestern) based on Hoechst 33342 DNA-staining (355nm laser, 450/50 emission filter),  
49  
50 592 thiazole orange RNA-staining (488nm laser, 525/50 emission filter) and DiIC<sub>1</sub>(5) mitochondrial  
51  
52 593 potential-signal (640nm laser, 670/30 emission filter). 100,000 single cells were counted per  
53  
54  
55  
56  
57  
58  
59  
60

1  
2  
3 594 sample and single events were distinguished from doublets using FSC-H and FSC-W gates. Data  
4  
5 595 was analyzed using FlowJo v10 (FlowJo, LLC, Ashland, OR). Infected RBCs with live parasites  
6  
7  
8 596 were defined as Hoechst/DNA-positive and DiIC<sub>1</sub>(5)/mitochondrial potential-positive according  
9  
10 597 to Grimberg <sup>78</sup>. Parasite stages were separated using Hoechst/DNA and thiazole orange/RNA  
11  
12 598 signals: ring stage parasites were defined as DNA-positive/RNA-negative; trophozoites and early  
13  
14  
15 599 schizonts were defined as <3N DNA-positive/RNA-positive; schizonts were defined at >3N DNA-  
16  
17 600 positive /RNA-positive.  
18  
19

#### 20 601 *Stage of parasite arrest*

21  
22

23 602 3D7 parasites were synchronized with 5% sorbitol two cycles prior to the experiment. On day 0, a  
24  
25 603 ring stage culture was set up at 3% parasitemia and 2% hematocrit. Half of the culture was seeded  
26  
27  
28 604 into a 24-well plate and drug added to measure the effect of inhibitors on ring stage parasites. On  
29  
30 605 day 1, late stage parasites from the remainder of the starting culture were re-fed and seeded into a  
31  
32 606 24-well plate to measure the effect of inhibitors on late stage parasites. At 0, 24, and 48 h after the  
33  
34  
35 607 addition of drug, thin blood smears were made and an aliquot of each sample was analyzed by  
36  
37 608 flow cytometry as described above.  
38  
39

#### 40 609 *Washout experiments*

41  
42

43 610 3D7 parasites were tightly synchronized to a 4-h window using 40/70% Percoll-sorbitol gradients  
44  
45 611 and seeded into multiple 96 well plates at 1% parasitemia and 2% hematocrit. At each time point,  
46  
47  
48 612 one plate was removed from the incubator and drug was added in fresh media in triplicate wells.  
49  
50 613 Parasites were resuspended by pipetting to ensure complete mixing and a thin blood smear was  
51  
52 614 made. After the 12 h treatment period, thin blood smears were made of sample wells. Media  
53  
54  
55 615 containing drug was removed and cells were washed 2x with fresh media. Fresh media was added  
56  
57  
58  
59  
60

1  
2  
3 616 and cells were thoroughly resuspended by pipetting prior to transferring 1:40 dilution of culture to  
4  
5 617 a second plate containing fresh complete media and RBCs at 2% hematocrit. Plates were then  
6  
7 618 returned to the incubator. At the defined time points, thin smears were made of sample wells and  
8  
9  
10 619 an aliquot of culture was transferred to a V-bottom 96-well plate for staining followed by flow  
11  
12 620 cytometry as described above.

### 15 621 *Plasmid construction*

18 622 Codon optimized PfJmj3 was synthesized by GenScript with BamHI and XbaI restriction sites  
19  
20 623 flanking the gene and cloned into pMAL-CHT expression plasmid <sup>79</sup> kindly provided by Sean  
21  
22 624 Prigge (Johns Hopkins Bloomberg School of Public Health). Catalytically dead PfJmj3 was  
23  
24 625 generated by site-directed mutagenesis using the following primers (for H342A: KM63 –  
25  
26 626 GCCGTGTGGATGGTTTGCCGAGGTGAAAAGCTTC and KM64 –  
27  
28 627 CGGAGCTGAAGCTTTTCACCTCGGCAAACCATCCAC; for H166A, D168A: KM65 –  
29  
30 628 CCAAAGTGAAGACATATCTGGCCCATGCTTACCATGAC and KM66 –  
31  
32 629 GCACATAGATATTGTCATGGTAAGCATGGGCCAGATATGTC). The entire open reading  
33  
34  
35 630 frame for both wild type and HDH>AAA plasmids were confirmed by DNA sequencing (UTSW  
36  
37 631 McDermott Sequencing Core). Plasmids were then transformed in Rosetta (DE3) Escherichia coli-  
38  
39 632 competent cells (Novagen, EMD Biosciences Inc., Madison, WI) for protein expression. For  
40  
41 633 protein purification, a single colony was grown in Luria Broth (Research Product International,  
42  
43 634 Mt. Prospect, IL) containing 100 µg/mL ampicillin and 35 µg/mL chloramphenicol.

### 49 635 *Protein purification*

52 636 Recombinant MBP-PfJmj3 overexpression was induced with 1 mM IPTG at 18° overnight. A cell  
53  
54 637 pellet from 8 L wild type was resuspended in 120 mL buffer A (50 mM HEPES, pH 7.5) with 150

1  
2  
3 638 mM NaCl containing with 0.2 mM phenylmethanesulfonyl fluoride and 3 protease inhibitors  
4  
5 639 tablets (Complete Mini; Roche, Mannheim, Germany) using a dounce homogenizer. Cells were  
6  
7 640 incubated with 200  $\mu\text{g}/\text{mL}$  lysozyme and 10  $\mu\text{g}/\text{mL}$  DNase at 4° for 1 h followed by lysis with by  
8  
9 641 tip sonicator (Heat Systems Inc., Farmingdale, NY) and then subjected to 50,000 x g centrifugation  
10  
11 642 at 4° for 30 min. The supernatant was loaded on a MBPTrap HP column (GE Healthcare, Uppsala,  
12  
13 643 Sweden). The column was washed with 50 column volumes of buffer A with 150 mM NaCl and  
14  
15 644 bound protein was eluted with 10 column volumes of buffer A containing 50 mM NaCl and 10  
16  
17 645 mM maltose. Protein containing fractions were pooled, diluted with buffer A, and loaded on a  
18  
19 646 HiTrap Q HP column (GE Healthcare). The column was washed with 50 column volumes of buffer  
20  
21 647 A containing 100 mM NaCl followed by 50 column volumes of buffer A with 300 mM NaCl.  
22  
23 648 Bound protein was eluted with 10 column volumes of buffer A containing 600 mM NaCl. The  
24  
25 649 eluted fractions with the desired protein were pooled and diluted with buffer A to a final  
26  
27 650 concentration of 150 mM NaCl with 20% glycerol and stored at -80° until use. Protein  
28  
29 651 concentrations were measured using the DC Protein Assay (BioRad, Hercules, CA). The  
30  
31 652 catalytically dead mutant protein was purified as above from 4 L.

### 32 33 653 *Succinate Assay*

34  
35 654 Succinate production from recombinant MBP-PfJmj3 was measured using the Succinate-Glo JmjC  
36  
37 655 Demethylase/Hydroxylase Assay (Promega, Madison, WI) according the manufacturer  
38  
39 656 instructions. Reaction mixtures (25  $\mu\text{L}$ ) containing 50 mM HEPES, pH 7.5, 100  $\mu\text{M}$  ascorbic acid,  
40  
41 657 10  $\mu\text{M}$   $\text{Fe}(\text{II})(\text{NH}_4)_2(\text{SO}_4)_2$ , and 10  $\mu\text{M}$  2-OG, except where noted, were set up in 96-well plate  
42  
43 658 (half area, white, flat bottom, non-binding; Corning, Kennebunk, ME). The reaction was initiated  
44  
45 659 by the addition of recombinant MBP-PfJmj3 protein (2  $\mu\text{M}$ ) and mixed for 2 m using a plate  
46  
47 660 shaker. For inhibitor reactions, enzyme was pre-incubated with 20  $\mu\text{M}$  ascorbic acid and 2  $\mu\text{M}$

1  
2  
3 661  $\text{Fe(II)(NH}_4)_2(\text{SO}_4)_2$  for 10 min on ice after which 10  $\mu\text{M}$  2-OG and inhibitor were added  
4  
5 662 simultaneously. All inhibitors were dissolved in DMSO at concentrations such that a total of 1  $\mu\text{L}$   
6  
7 663 was added to each reaction. Inhibition curves were performed using 3 fold serial dilutions starting  
8  
9 664 with 15  $\mu\text{M}$  (to 0.18  $\mu\text{M}$ ). After incubation for 1 h at room temperature, 25  $\mu\text{L}$  of Succinate  
10  
11 665 Detection Reagent I was added to each well and mixed for 2 m using a plate shaker. Following  
12  
13 666 incubation for 1 h at room temperature, 50  $\mu\text{L}$  of Succinate Detection Reagent II was added to  
14  
15 667 each well and mixed for 30 s. Luminescence was measured after 10 m on a microplate reader  
16  
17 668 (FLUOstar Omega; BMG Labtech, Cary, NC). Independent experiments for each inhibitor were  
18  
19 669 performed with different batches of enzyme: JIB-04 E (n = 5), JIB-04 Z (n = 2), GSK-J4 (n = 4),  
20  
21 670 ML324 (n = 4), and SD-70 (n = 4). Non-linear regression curves ([Inhibitor] vs. response - Variable  
22  
23 671 slope (four parameters)) were fit using GraphPad Prism version 8.  
24  
25  
26  
27  
28

29 672 *Mass spectrometry analysis for histone PTMs*  
30  
31

32 673 3D7 parasites were tightly synchronized to a 4 h window as above and seeded at 4% parasitemia  
33  
34 674 and 2% hematocrit. Drug was added at 29 hpi. After 6 h, infected RBCs were pelleted and  
35  
36 675 immediately frozen in liquid nitrogen. After thawing, parasites were isolated from RBCs using  
37  
38 676 0.05% saponin in cold PBS and subsequently washed 3x in cold PBS. Histones were extracted  
39  
40 677 using the EpiQuik Total Histone Extraction kit (Epigentek, Farmingdale, NY) followed by TCA  
41  
42 678 precipitation. A portion of the histone extracts were run on a 15% SDS-PAGE gel and visualized  
43  
44 679 with Quick Coomassie Stain (Protein Ark, Sheffield, United Kingdom) to determine purity and  
45  
46 680 concentration. Histones were prepared for mass spectrometry by chemical derivatization using  
47  
48 681 propionic anhydride and digested to peptides with trypsin, followed by another round of  
49  
50 682 derivatization. Peptides were desalted using C18 stage-tips and about 1-2  $\mu\text{g}$  peptides were  
51  
52 683 analyzed using an EASY-nLC nanoHPLC (Thermo Scientific, Odense, Denmark) coupled with a  
53  
54  
55  
56  
57  
58  
59  
60

1  
2  
3 684 Q-Exactive mass spectrometer (Thermo Fisher Scientific, Bremen, Germany). HPLC gradients  
4  
5 685 and mass spectrometry parameters were defined previously <sup>80</sup>. To facilitate MS/MS-based  
6  
7 686 quantification, both data-dependent acquisition and targeted acquisition for isobaric peptides were  
8  
9  
10 687 included. The relative abundance of histone H3 and H4 peptides were calculated by using  
11  
12 688 EpiProfile <sup>81</sup>.

### 15 689 *RNA sequencing and analysis pipeline*

17  
18 690 3D7 parasites were tightly synchronized to a 3 h window using Percoll-sorbitol gradients. Parasites  
19  
20 691 were seeded into 6-well plates at 4% parasitemia and 2% hematocrit. At 29 hpi, drug was added  
21  
22 692 to each well with a final DMSO concentration of 0.04%. Four replicates were performed for each  
23  
24 693 treatment. One set of cultures was harvested immediately corresponding to 0 h treatment and the  
25  
26 694 remaining cultures were harvested after a 6 h incubation. Parasite culture was passed through a  
27  
28 695 Plasmodipur filter (EuroProxima, Arnhem, Netherlands) to remove residual white blood cells.  
29  
30 696 Parasite pellets were immediately lysed in Trizol LS Reagent (ThermoFisher Scientific) and  
31  
32 697 subsequently snap frozen in liquid nitrogen. RNA was isolated according to manufacturers'  
33  
34 698 instructions and precipitated in the presence of linear acrylamide (Amresco, Solon, OH). Samples  
35  
36 699 were prepared from 2 µg of RNA using the Illumina (San Diego, CA) Tru-stranded mRNA library  
37  
38 700 kit according to manufacturers' directions. RNA and library quality were validated on an Agilent  
39  
40 701 2100 Bioanalyzer prior to sequencing on an Illumina NextSeq 500 (McDermott Next Generation  
41  
42 702 Sequencing Core, UT Southwestern) at an average of 37,000,000 reads per sample. Raw reads  
43  
44 703 were processed (McDermott Center Bioinformatics Core, UT Southwestern) and aligned (STAR  
45  
46 704 aligner) to the *P. falciparum* 3D7 transcriptome (PlasmoDB v. 34) <sup>16</sup>. Unique transcripts mapped  
47  
48 705 to an average of 94% of the transcriptome. Expressed genes were defined as genes with an average  
49  
50 706 expression higher than 0.1 RPKM across the four replicates. Differential expression analysis was

1  
2  
3 707 performed using EdgeR (Bioconductor) <sup>82-83</sup>. We selected genes with a >1.5-fold difference  
4  
5 708 between JIB-04 E and either vehicle or JIB-04 Z treatment groups, and a FDR of <0.05 for further  
6  
7 709 analysis. Gene ontology (GO) enrichment analysis was performed at PlasmoDB.org <sup>16</sup> and Malaria  
8  
9 710 Parasite Metabolic Pathways (MPMP), <http://mpmp.huji.ac.il/>. Heatmaps and Venn diagrams were  
10  
11 711 generated using Morpheus (<https://software.broadinstitute.org/morpheus>; Broad Institute) and  
12  
13 712 BioVenn <sup>84</sup>, respectively.

### 14 15 713 *qRT-PCR*

16  
17  
18  
19  
20 714 RNA was purified using a Trizol LS (ThermoFisher Scientific) extraction method. Approximately  
21  
22 715 2 µg of RNA was treated with DNase I (Roche) prior to reverse transcription using the High  
23  
24 716 Capacity cDNA Reverse Transcription kit (Applied Biosystems, Foster City, CA). Quantitative  
25  
26 717 PCR (qPCR) was performed in triplicate wells using SYBR Green ER qPCR SuperMix  
27  
28 718 (Invitrogen, Carlsbad, CA). qPCR reactions were run on an ABI 7300 Real-time PCR System and  
29  
30 719 analyzed with QuantStudio Real Time PCR software (Applied Biosystems). The  $\Delta\Delta C_t$  method  
31  
32 720 was used to compute relative mRNA expression with serine tRNA ligase (*PF3D7\_0717700*) as a  
33  
34 721 reference gene. The list of primers used is in Table S2.

### 35 36 37 38 39 722 *Bioinformatics analysis*

40  
41  
42 723 We compared the differentially expressed gene list to various publicly available data sets. We  
43  
44 724 defined PfBDP1 targets (from Table S6 in <sup>51</sup>) as those genes with peak ChIP enrichment in either  
45  
46 725 trophozoite or schizont stages and PfAP2-I targets (from Table S2 in <sup>50</sup>) as those genes with  
47  
48 726 trimmed peak ChIP enrichment schizonts. We compared our list of differentially expressed genes  
49  
50 727 from JIB-04 E-treated and PbAP2-SP knockout parasites <sup>55</sup> using a cut of 1.5-fold and FDR<0.05.  
51  
52 728 *P. falciparum* orthologs of *P. berghei* gene IDs were determined using PlasmoDB <sup>16</sup>. Using  
53  
54  
55  
56  
57  
58  
59  
60

1  
2  
3 729 PlasmoDB, we searched the RNAseq transcriptomes of asexual and sexual stages from Lopez-  
4  
5 730 Barragan *et al.* <sup>18</sup> for genes with >5-fold expression in stage II or V gametocytes, or ookinetes  
6  
7  
8 731 compared to trophozoites or schizonts. We stringently defined stage specific genes as those with  
9  
10 732 <5 FPKM in trophozoites and schizonts and >5-fold expression in gametocytes or ookinetes. We  
11  
12 733 further cross-referenced these genes with the male and female gametocyte transcriptomes from  
13  
14 734 Lasonder *et al.* <sup>54</sup>. Venn diagrams were generated using BioVenn <sup>84</sup>, and Fisher t test and  
15  
16 735 hypergeometric distribution of overlap was performed using R i386 version 3.5.3.  
17  
18  
19

20 736 *Data Availability*  
21  
22

23 737 All RNAseq datasets have been deposited under the GEO accession number GSE117307.  
24  
25  
26  
27  
28  
29  
30  
31  
32  
33  
34  
35  
36  
37  
38  
39  
40  
41  
42  
43  
44  
45  
46  
47  
48  
49  
50  
51  
52  
53  
54  
55  
56  
57  
58  
59  
60

1  
2  
3 738 **Ancillary Information**  
4

5  
6 739 **Supporting information:**  
7

8  
9 740 Figure S1-S6 – supplemental figures and legends  
10

11  
12 741 Table S1 – Structures of Jumonji histone demethylase inhibitors used in this study  
13

14  
15 742 Table S2 – list of QRT-PCR primer sequences  
16

17  
18 743 Table S3 – supplemental data relating to Figure 5  
19

20  
21 744 Table S4 – functional gene groups and statistical analysis related to Figures 5 and 6  
22

23  
24 745 **Corresponding Author Information:** [elisabeth.martinez@utsouthwestern.edu](mailto:elisabeth.martinez@utsouthwestern.edu)  
25  
26

27  
28 746 **Acknowledgements:** We are deeply grateful to Dr. Margaret Phillips for invaluable resources and  
29  
30 747 suggestions, and Dr. Jacqueline Njoroge for initial observations. We are grateful to Nicholas Loof  
31  
32 748 and the Moody Foundation Flow Cytometry Core for help with establishing the flow cytometry  
33  
34 749 set up, and Dr. Arun Radhakrishnan for his assistance in the protein purification of PfJmj3. Thanks  
35  
36 750 to Drs. Tram Anh Tran and Lei Wang for general project support. This work was partly funded by  
37  
38 751 The Welch Foundation (I-1878 to EDM), by the Alfred & Kathryn Gilman Family Giving Fund  
39  
40 752 (to KAM and EDM), by the John P. Perkins, Ph.D. Distinguished Professorship in Biomedical  
41  
42 753 Science Endowment (to EDM), by the NIH (R21AI139408 to EDM and R01AI141965 to BK), by  
43  
44 754 CPRIT (RP160493 to EDM), by Alice Bohmfalk Charitable Trust Research Grant (to BK), and by  
45  
46 755 the Jacques Cohenca Predoctoral Fellowship (to CN).  
47  
48  
49  
50  
51

52 756 **Abbreviations Used:** *Pf*, *Plasmodium falciparum*; *Pb*, *Plasmodium berghei*; JmjC, Jumonji C;  
53  
54 757 RBC, red blood cell; 2-OG, 2-oxoglutarate; IDC, intraerythrocytic development cycle; KDM,  
55  
56  
57  
58  
59  
60

1  
2  
3  
4  
5  
6  
7  
8  
9  
10  
11  
12  
13  
14  
15  
16  
17  
18  
19  
20  
21  
22  
23  
24  
25  
26  
27  
28  
29  
30  
31  
32  
33  
34  
35  
36  
37  
38  
39  
40  
41  
42  
43  
44  
45  
46  
47  
48  
49  
50  
51  
52  
53  
54  
55  
56  
57  
58  
59  
60

758 histone lysine demethylase; EC, effective concentration; GC, gametocyte; hpi, hours post invasion;  
759 GO, gene ontology; BDP1, bromodomain protein 1; KMT, histone lysine methyltransferase

760 **References**

- 761 1. WHO, World malaria report 2018. **2018**.
- 762 2. Merrick, C. J.; Duraisingh, M. T., Epigenetics in Plasmodium: what do we really know? *Eukaryotic*  
763 *cell* **2010**, *9* (8), 1150-8.
- 764 3. Rovira-Graells, N.; Gupta, A. P.; Planet, E.; Crowley, V. M.; Mok, S.; Ribas de Pouplana, L.; Preiser,  
765 P. R.; Bozdech, Z.; Cortes, A., Transcriptional variation in the malaria parasite Plasmodium falciparum.  
766 *Genome research* **2012**, *22* (5), 925-38.
- 767 4. Flueck, C.; Bartfai, R.; Volz, J.; Niederwieser, I.; Salcedo-Amaya, A. M.; Alako, B. T.; Ehlgren, F.;  
768 Ralph, S. A.; Cowman, A. F.; Bozdech, Z.; Stunnenberg, H. G.; Voss, T. S., Plasmodium falciparum  
769 heterochromatin protein 1 marks genomic loci linked to phenotypic variation of exported virulence  
770 factors. *PLoS pathogens* **2009**, *5* (9), e1000569.
- 771 5. Lopez-Rubio, J. J.; Mancio-Silva, L.; Scherf, A., Genome-wide analysis of heterochromatin  
772 associates clonally variant gene regulation with perinuclear repressive centers in malaria parasites. *Cell*  
773 *host & microbe* **2009**, *5* (2), 179-90.
- 774 6. Brancucci, N. M. B.; Bertschi, N. L.; Zhu, L.; Niederwieser, I.; Chin, W. H.; Wampfler, R.;  
775 Freymond, C.; Rottmann, M.; Felger, I.; Bozdech, Z.; Voss, T. S., Heterochromatin protein 1 secures  
776 survival and transmission of malaria parasites. *Cell Host Microbe* **2014**, *16* (2), 165-176.
- 777 7. Deitsch, K. W.; Dzikowski, R., Variant Gene Expression and Antigenic Variation by Malaria  
778 Parasites. *Annu Rev Microbiol* **2017**, *71*, 625-641.
- 779 8. Swamy, L.; Amulic, B.; Deitsch, K. W., Plasmodium falciparum var gene silencing is determined  
780 by cis DNA elements that form stable and heritable interactions. *Eukaryot Cell* **2011**, *10* (4), 530-9.
- 781 9. Duraisingh, M. T.; Horn, D., Epigenetic Regulation of Virulence Gene Expression in Parasitic  
782 Protozoa. *Cell host & microbe* **2016**, *19* (5), 629-40.
- 783 10. Merrick, C. J.; Huttenhower, C.; Buckee, C.; Amambua-Ngwa, A.; Gomez-Escobar, N.; Walther,  
784 M.; Conway, D. J.; Duraisingh, M. T., Epigenetic dysregulation of virulence gene expression in severe  
785 Plasmodium falciparum malaria. *The Journal of infectious diseases* **2012**, *205* (10), 1593-600.
- 786 11. Jiang, L.; Lopez-Barragan, M. J.; Jiang, H.; Mu, J.; Gaur, D.; Zhao, K.; Felsenfeld, G.; Miller, L. H.,  
787 Epigenetic control of the variable expression of a Plasmodium falciparum receptor protein for  
788 erythrocyte invasion. *Proceedings of the National Academy of Sciences of the United States of America*  
789 **2010**, *107* (5), 2224-9.
- 790 12. Markolovic, S.; Leissing, T. M.; Chowdhury, R.; Wilkins, S. E.; Lu, X.; Schofield, C. J., Structure-  
791 function relationships of human JmjC oxygenases-demethylases versus hydroxylases. *Curr Opin Struct*  
792 *Biol* **2016**, *41*, 62-72.
- 793 13. Herr, C. Q.; Hausinger, R. P., Amazing Diversity in Biochemical Roles of Fe(II)/2-Oxoglutarate  
794 Oxygenases. *Trends in biochemical sciences* **2018**, *43* (7), 517-532.
- 795 14. Cui, L. W.; Fan, Q.; Cui, L.; Miao, J., Histone lysine methyltransferases and demethylases in  
796 Plasmodium falciparum. *Int J Parasitol* **2008**, *38* (10), 1083-1097.
- 797 15. Jiang, L.; Mu, J.; Zhang, Q.; Ni, T.; Srinivasan, P.; Rayavara, K.; Yang, W.; Turner, L.; Lavstsen, T.;  
798 Theander, T. G.; Peng, W.; Wei, G.; Jing, Q.; Wakabayashi, Y.; Bansal, A.; Luo, Y.; Ribeiro, J. M.; Scherf, A.;  
799 Aravind, L.; Zhu, J.; Zhao, K.; Miller, L. H., PfSETvs methylation of histone H3K36 represses virulence  
800 genes in Plasmodium falciparum. *Nature* **2013**, *499* (7457), 223-7.
- 801 16. Aurrecochea, C.; Brestelli, J.; Brunk, B. P.; Dommer, J.; Fischer, S.; Gajria, B.; Gao, X.; Gingle, A.;  
802 Grant, G.; Harb, O. S.; Heiges, M.; Innamorato, F.; Iodice, J.; Kissinger, J. C.; Kraemer, E.; Li, W.; Miller, J.  
803 A.; Nayak, V.; Pennington, C.; Pinney, D. F.; Roos, D. S.; Ross, C.; Stoeckert, C. J., Jr.; Treatman, C.; Wang,  
804 H., PlasmoDB: a functional genomic database for malaria parasites. *Nucleic acids research* **2009**, *37*  
805 (Database issue), D539-43.

- 1  
2  
3 806 17. Bartfai, R.; Hoeijmakers, W. A.; Salcedo-Amaya, A. M.; Smits, A. H.; Janssen-Megens, E.; Kaan, A.;  
4 807 Treeck, M.; Gilberger, T. W.; Francoijs, K. J.; Stunnenberg, H. G., H2A.Z demarcates intergenic regions of  
5 808 the plasmodium falciparum epigenome that are dynamically marked by H3K9ac and H3K4me3. *PLoS*  
6 809 *pathogens* **2010**, *6* (12), e1001223.
- 8 810 18. Lopez-Barragan, M. J.; Lemieux, J.; Quinones, M.; Williamson, K. C.; Molina-Cruz, A.; Cui, K.;  
9 811 Barillas-Mury, C.; Zhao, K.; Su, X. Z., Directional gene expression and antisense transcripts in sexual and  
10 812 asexual stages of Plasmodium falciparum. *BMC genomics* **2011**, *12*, 587.
- 11 813 19. Young, J. A.; Fivelman, Q. L.; Blair, P. L.; de la Vega, P.; Le Roch, K. G.; Zhou, Y.; Carucci, D. J.;  
12 814 Baker, D. A.; Winzeler, E. A., The Plasmodium falciparum sexual development transcriptome: a  
13 815 microarray analysis using ontology-based pattern identification. *Molecular and biochemical parasitology*  
14 816 **2005**, *143* (1), 67-79.
- 15 817 20. Zhang, M.; Wang, C.; Otto, T. D.; Oberstaller, J.; Liao, X.; Adapa, S. R.; Udenze, K.; Bronner, I. F.;  
16 818 Casandra, D.; Mayho, M.; Brown, J.; Li, S.; Swanson, J.; Rayner, J. C.; Jiang, R. H. Y.; Adams, J. H.,  
17 819 Uncovering the essential genes of the human malaria parasite Plasmodium falciparum by saturation  
18 820 mutagenesis. *Science* **2018**, *360* (6388).
- 20 821 21. Hojfeldt, J. W.; Agger, K.; Helin, K., Histone lysine demethylases as targets for anticancer  
21 822 therapy. *Nat Rev Drug Discov* **2013**, *12* (12), 917-30.
- 22 823 22. Maes, T.; Carceller, E.; Salas, J.; Ortega, A.; Buesa, C., Advances in the development of histone  
23 824 lysine demethylase inhibitors. *Curr Opin Pharmacol* **2015**, *23*, 52-60.
- 24 825 23. Wang, L.; Chang, J.; Varghese, D.; Dellinger, M.; Kumar, S.; Best, A. M.; Ruiz, J.; Bruick, R.; Pena-  
25 826 Llopis, S.; Xu, J.; Babinski, D. J.; Frantz, D. E.; Brekken, R. A.; Quinn, A. M.; Simeonov, A.; Easmon, J.;  
26 827 Martinez, E. D., A small molecule modulates Jumonji histone demethylase activity and selectively  
27 828 inhibits cancer growth. *Nature communications* **2013**, *4*, 2035.
- 29 829 24. Bayo, J.; Dalvi, M. P.; Martinez, E. D., Successful strategies in the discovery of small-molecule  
30 830 epigenetic modulators with anticancer potential. *Future Med Chem* **2015**, *7* (16), 2243-61.
- 31 831 25. Cascella, B.; Lee, S. G.; Singh, S.; Jez, J. M.; Mirica, L. M., The small molecule JIB-04 disrupts O2  
32 832 binding in the Fe-dependent histone demethylase KDM4A/JMJD2A. *Chemical communications*  
33 833 *(Cambridge, England)* **2017**, *53* (13), 2174-2177.
- 34 834 26. Horton, J. R.; Liu, X.; Gale, M.; Wu, L.; Shanks, J. R.; Zhang, X.; Webber, P. J.; Bell, J. S.; Kales, S.  
35 835 C.; Mott, B. T.; Rai, G.; Jansen, D. J.; Henderson, M. J.; Urban, D. J.; Hall, M. D.; Simeonov, A.; Maloney, D.  
36 836 J.; Johns, M. A.; Fu, H.; Jadhav, A.; Vertino, P. M.; Yan, Q.; Cheng, X., Structural Basis for KDM5A Histone  
37 837 Lysine Demethylase Inhibition by Diverse Compounds. *Cell Chem Biol* **2016**, *23* (7), 769-81.
- 39 838 27. Kruidenier, L.; Chung, C. W.; Cheng, Z.; Liddle, J.; Che, K.; Joberty, G.; Bantscheff, M.; Bountra, C.;  
40 839 Bridges, A.; Diallo, H.; Eberhard, D.; Hutchinson, S.; Jones, E.; Katso, R.; Leveridge, M.; Mander, P. K.;  
41 840 Mosley, J.; Ramirez-Molina, C.; Rowland, P.; Schofield, C. J.; Sheppard, R. J.; Smith, J. E.; Swales, C.;  
42 841 Tanner, R.; Thomas, P.; Tumber, A.; Drewes, G.; Oppermann, U.; Patel, D. J.; Lee, K.; Wilson, D. M., A  
43 842 selective jumonji H3K27 demethylase inhibitor modulates the proinflammatory macrophage response.  
44 843 *Nature* **2012**, *488* (7411), 404-8.
- 46 844 28. Thinnes, C. C.; England, K. S.; Kawamura, A.; Chowdhury, R.; Schofield, C. J.; Hopkinson, R. J.,  
47 845 Targeting histone lysine demethylases - progress, challenges, and the future. *Biochimica et biophysica*  
48 846 *acta* **2014**, *1839* (12), 1416-32.
- 49 847 29. Vinogradova, M.; Gehling, V. S.; Gustafson, A.; Arora, S.; Tindell, C. A.; Wilson, C.; Williamson, K.  
50 848 E.; Guler, G. D.; Gangurde, P.; Manieri, W.; Busby, J.; Flynn, E. M.; Lan, F.; Kim, H. J.; Odate, S.; Cochran,  
51 849 A. G.; Liu, Y.; Wongchenko, M.; Yang, Y.; Cheung, T. K.; Maile, T. M.; Lau, T.; Costa, M.; Hegde, G. V.;  
52 850 Jackson, E.; Pitti, R.; Arnott, D.; Bailey, C.; Bellon, S.; Cummings, R. T.; Albrecht, B. K.; Harmange, J. C.;  
53 851 Kiefer, J. R.; Trojer, P.; Classon, M., An inhibitor of KDM5 demethylases reduces survival of drug-tolerant  
54 852 cancer cells. *Nat Chem Biol* **2016**, *12* (7), 531-8.

- 1  
2  
3 853 30. Smilkstein, M.; Sriwilaijaroen, N.; Kelly, J. X.; Wilairat, P.; Riscoe, M., Simple and Inexpensive  
4 854 Fluorescence-Based Technique for High-Throughput Antimalarial Drug Screening. *Antimicrobial agents*  
5 855 *and chemotherapy* **2004**, *48* (5), 1803-1806.
- 6 856 31. Ntziachristos, P.; Tsigos, A.; Welstead, G. G.; Trimarchi, T.; Bakogianni, S.; Xu, L.; Loizou, E.;  
7 857 Holmfeldt, L.; Strikoudis, A.; King, B.; Mullenders, J.; Becksfort, J.; Nedjic, J.; Paietta, E.; Tallman, M. S.;  
8 858 Rowe, J. M.; Tonon, G.; Satoh, T.; Kruidenier, L.; Prinjha, R.; Akira, S.; Van Vlierberghe, P.; Ferrando, A. A.;  
9 859 Jaenisch, R.; Mullighan, C. G.; Aifantis, I., Contrasting roles of histone 3 lysine 27 demethylases in acute  
10 860 lymphoblastic leukaemia. *Nature* **2014**, *514* (7523), 513-7.
- 11 861 32. Dalvi, M. P.; Wang, L.; Zhong, R.; Kollipara, R. K.; Park, H.; Bayo, J.; Yenerall, P.; Zhou, Y.;  
12 862 Timmons, B. C.; Rodriguez-Canales, J.; Behrens, C.; Mino, B.; Villalobos, P.; Parra, E. R.; Suraokar, M.;  
13 863 Pataer, A.; Swisher, S. G.; Kalhor, N.; Bhanu, N. V.; Garcia, B. A.; Heymach, J. V.; Coombes, K.; Xie, Y.;  
14 864 Girard, L.; Gazdar, A. F.; Kittler, R.; Wistuba, II; Minna, J. D.; Martinez, E. D., Taxane-Platin-Resistant Lung  
15 865 Cancers Co-develop Hypersensitivity to JumonjiC Demethylase Inhibitors. *Cell Rep* **2017**, *19* (8), 1669-  
16 866 1684.
- 17 867 33. Heinemann, B.; Nielsen, J. M.; Hudlebusch, H. R.; Lees, M. J.; Larsen, D. V.; Boesen, T.; Labelle,  
18 868 M.; Gerlach, L. O.; Birk, P.; Helin, K., Inhibition of demethylases by GSK-J1/J4. *Nature* **2014**, *514* (7520),  
19 869 E1-2.
- 20 870 34. Hamada, S.; Suzuki, T.; Mino, K.; Koseki, K.; Oehme, F.; Flamme, I.; Ozasa, H.; Itoh, Y.;  
21 871 Ogasawara, D.; Komaarashi, H.; Kato, A.; Tsumoto, H.; Nakagawa, H.; Hasegawa, M.; Sasaki, R.;  
22 872 Mizukami, T.; Miyata, N., Design, synthesis, enzyme-inhibitory activity, and effect on human cancer cells  
23 873 of a novel series of jumonji domain-containing protein 2 histone demethylase inhibitors. *J Med Chem*  
24 874 **2010**, *53* (15), 5629-38.
- 25 875 35. Cucchiara, V.; Yang, J. C.; Mirone, V.; Gao, A. C.; Rosenfeld, M. G.; Evans, C. P., Epigenomic  
26 876 Regulation of Androgen Receptor Signaling: Potential Role in Prostate Cancer Therapy. *Cancers* **2017**, *9*  
27 877 (1).
- 28 878 36. Johansson, C.; Velupillai, S.; Tumber, A.; Szykowska, A.; Hookway, E. S.; Nowak, R. P.; Strain-  
29 879 Damerell, C.; Gileadi, C.; Philpott, M.; Burgess-Brown, N.; Wu, N.; Kopec, J.; Nuzzi, A.; Steuber, H.; Egner,  
30 880 U.; Badock, V.; Munro, S.; LaThangue, N. B.; Westaway, S.; Brown, J.; Athanasou, N.; Prinjha, R.;  
31 881 Brennan, P. E.; Oppermann, U., Structural analysis of human KDM5B guides histone demethylase  
32 882 inhibitor development. *Nat Chem Biol* **2016**, *12* (7), 539-45.
- 33 883 37. Delves, M. J.; Straschil, U.; Ruecker, A.; Miguel-Blanco, C.; Marques, S.; Dufour, A. C.; Baum, J.;  
34 884 Sinden, R. E., Routine in vitro culture of *P. falciparum* gametocytes to evaluate novel transmission-  
35 885 blocking interventions. *Nat Protoc* **2016**, *11* (9), 1668-80.
- 36 886 38. Ruecker, A.; Mathias, D. K.; Straschil, U.; Churcher, T. S.; Dinglasan, R. R.; Leroy, D.; Sinden, R. E.;  
37 887 Delves, M. J., A male and female gametocyte functional viability assay to identify biologically relevant  
38 888 malaria transmission-blocking drugs. *Antimicrobial agents and chemotherapy* **2014**, *58* (12), 7292-302.
- 39 889 39. Delves, M. J.; Ruecker, A.; Straschil, U.; Lelievre, J.; Marques, S.; Lopez-Barragan, M. J.; Herreros,  
40 890 E.; Sinden, R. E., Male and female *Plasmodium falciparum* mature gametocytes show different responses  
41 891 to antimalarial drugs. *Antimicrobial agents and chemotherapy* **2013**, *57* (7), 3268-74.
- 42 892 40. Hancock, R. L.; Abboud, M. I.; Smart, T. J.; Flashman, E.; Kawamura, A.; Schofield, C. J.;  
43 893 Hopkinson, R. J., Lysine-241 Has a Role in Coupling 2OG Turnover with Substrate Oxidation During  
44 894 KDM4-Catalysed Histone Demethylation. *ChemBiochem : a European journal of chemical biology* **2018**,  
45 895 *19* (9), 917-921.
- 46 896 41. Lopez-Rubio, J. J.; Gontijo, A. M.; Nunes, M. C.; Issar, N.; Hernandez Rivas, R.; Scherf, A., 5'  
47 897 flanking region of var genes nucleate histone modification patterns linked to phenotypic inheritance of  
48 898 virulence traits in malaria parasites. *Molecular microbiology* **2007**, *66* (6), 1296-305.

- 1  
2  
3 899 42. Chookajorn, T.; Dzikowski, R.; Frank, M.; Li, F.; Jiwani, A. Z.; Hartl, D. L.; Deitsch, K. W., Epigenetic  
4 900 memory at malaria virulence genes. *Proceedings of the National Academy of Sciences of the United*  
5 901 *States of America* **2007**, *104* (3), 899-902.
- 6 902 43. Karmodiya, K.; Pradhan, S. J.; Joshi, B.; Jangid, R.; Reddy, P. C.; Galande, S., A comprehensive  
7 903 epigenome map of *Plasmodium falciparum* reveals unique mechanisms of transcriptional regulation and  
8 904 identifies H3K36me2 as a global mark of gene suppression. *Epigenetics Chromatin* **2015**, *8*, 32.
- 9 905 44. Ukaegbu, U. E.; Kishore, S. P.; Kwiatkowski, D. L.; Pandarinath, C.; Dahan-Pasternak, N.;  
10 906 Dzikowski, R.; Deitsch, K. W., Recruitment of PfSET2 by RNA polymerase II to variant antigen encoding  
11 907 loci contributes to antigenic variation in *P. falciparum*. *PLoS pathogens* **2014**, *10* (1), e1003854.
- 12 908 45. Gupta, A. P.; Chin, W. H.; Zhu, L.; Mok, S.; Luah, Y. H.; Lim, E. H.; Bozdech, Z., Dynamic epigenetic  
13 909 regulation of gene expression during the life cycle of malaria parasite *Plasmodium falciparum*. *PLoS*  
14 910 *pathogens* **2013**, *9* (2), e1003170.
- 15 911 46. Rai, R.; Zhu, L.; Chen, H.; Gupta, A. P.; Sze, S. K.; Zheng, J.; Ruedl, C.; Bozdech, Z.; Featherstone,  
16 912 M., Genome-wide analysis in *Plasmodium falciparum* reveals early and late phases of RNA polymerase II  
17 913 occupancy during the infectious cycle. *BMC genomics* **2014**, *15*, 959.
- 18 914 47. Chaal, B. K.; Gupta, A. P.; Wastuwidyaningtyas, B. D.; Luah, Y. H.; Bozdech, Z., Histone  
19 915 deacetylases play a major role in the transcriptional regulation of the *Plasmodium falciparum* life cycle.  
20 916 *PLoS pathogens* **2010**, *6* (1), e1000737.
- 21 917 48. Hu, G.; Cabrera, A.; Kono, M.; Mok, S.; Chaal, B. K.; Haase, S.; Engelberg, K.; Cheemadan, S.;  
22 918 Spielmann, T.; Preiser, P. R.; Gilberger, T. W.; Bozdech, Z., Transcriptional profiling of growth  
23 919 perturbations of the human malaria parasite *Plasmodium falciparum*. *Nature biotechnology* **2010**, *28* (1),  
24 920 91-8.
- 25 921 49. Bozdech, Z.; Llinas, M.; Pulliam, B. L.; Wong, E. D.; Zhu, J.; DeRisi, J. L., The transcriptome of the  
26 922 intraerythrocytic developmental cycle of *Plasmodium falciparum*. *PLoS biology* **2003**, *1* (1), E5.
- 27 923 50. Santos, J. M.; Josling, G.; Ross, P.; Joshi, P.; Orchard, L.; Campbell, T.; Schieler, A.; Cristea, I. M.;  
28 924 Llinas, M., Red Blood Cell Invasion by the Malaria Parasite Is Coordinated by the PfAP2-I Transcription  
29 925 Factor. *Cell host & microbe* **2017**, *21* (6), 731-741.e10.
- 30 926 51. Josling, G. A.; Petter, M.; Oehring, S. C.; Gupta, A. P.; Dietz, O.; Wilson, D. W.; Schubert, T.;  
31 927 Langst, G.; Gilson, P. R.; Crabb, B. S.; Moes, S.; Jenoe, P.; Lim, S. W.; Brown, G. V.; Bozdech, Z.; Voss, T. S.;  
32 928 Duffy, M. F., A *Plasmodium falciparum* Bromodomain Protein Regulates Invasion Gene Expression. *Cell*  
33 929 *host & microbe* **2015**, *17* (6), 741-51.
- 34 930 52. Leykauf, K.; Treeck, M.; Gilson, P. R.; Nebl, T.; Braulke, T.; Cowman, A. F.; Gilberger, T. W.; Crabb,  
35 931 B. S., Protein kinase a dependent phosphorylation of apical membrane antigen 1 plays an important role  
36 932 in erythrocyte invasion by the malaria parasite. *PLoS pathogens* **2010**, *6* (6), e1000941.
- 37 933 53. Lasonder, E.; Green, J. L.; Camarda, G.; Talabani, H.; Holder, A. A.; Langsley, G.; Alano, P., The  
38 934 *Plasmodium falciparum* schizont phosphoproteome reveals extensive phosphatidylinositol and cAMP-  
39 935 protein kinase A signaling. *J Proteome Res* **2012**, *11* (11), 5323-37.
- 40 936 54. Lasonder, E.; Rijpma, S. R.; van Schaijk, B. C.; Hoeijmakers, W. A.; Kensche, P. R.; Gresnigt, M. S.;  
41 937 Italiaander, A.; Vos, M. W.; Woestenenk, R.; Bousema, T.; Mair, G. R.; Khan, S. M.; Janse, C. J.; Bartfai, R.;  
42 938 Sauerwein, R. W., Integrated transcriptomic and proteomic analyses of *P. falciparum* gametocytes:  
43 939 molecular insight into sex-specific processes and translational repression. *Nucleic acids research* **2016**,  
44 940 *44* (13), 6087-101.
- 45 941 55. Modrzynska, K.; Pfander, C.; Chappell, L.; Yu, L.; Suarez, C.; Dundas, K.; Gomes, A. R.; Goulding,  
46 942 D.; Rayner, J. C.; Choudhary, J.; Billker, O., A Knockout Screen of ApiAP2 Genes Reveals Networks of  
47 943 Interacting Transcriptional Regulators Controlling the *Plasmodium* Life Cycle. *Cell host & microbe* **2017**,  
48 944 *21* (1), 11-22.
- 49 945 56. Malmquist, N. A.; Moss, T. A.; Mecheri, S.; Scherf, A.; Fuchter, M. J., Small-molecule histone  
50 946 methyltransferase inhibitors display rapid antimalarial activity against all blood stage forms in

- 1  
2  
3 947 Plasmodium falciparum. *Proceedings of the National Academy of Sciences of the United States of*  
4 948 *America* **2012**, *109* (41), 16708-13.
- 5 949 57. Malmquist, N. A.; Sundriyal, S.; Caron, J.; Chen, P.; Witkowski, B.; Menard, D.; Suwanarusk, R.;  
6 950 Renia, L.; Nosten, F.; Jimenez-Diaz, M. B.; Angulo-Barturen, I.; Santos Martinez, M.; Ferrer, S.; Sanz, L.  
7 951 M.; Gamo, F. J.; Wittlin, S.; Duffy, S.; Avery, V. M.; Ruecker, A.; Delves, M. J.; Sinden, R. E.; Fuchter, M. J.;  
8 952 Scherf, A., Histone methyltransferase inhibitors are orally bioavailable, fast-acting molecules with  
9 953 activity against different species causing malaria in humans. *Antimicrobial agents and chemotherapy*  
10 954 **2015**, *59* (2), 950-9.
- 11 955 58. Sundriyal, S.; Malmquist, N. A.; Caron, J.; Blundell, S.; Liu, F.; Chen, X.; Srimongkolpithak, N.; Jin,  
12 956 J.; Charman, S. A.; Scherf, A.; Fuchter, M. J., Development of Diaminoquinazoline Histone Lysine  
13 957 Methyltransferase Inhibitors as Potent Blood-Stage Antimalarial Compounds. *ChemMedChem* **2014**.
- 14 958 59. Andrews, K. T.; Gupta, A. P.; Tran, T. N.; Fairlie, D. P.; Gobert, G. N.; Bozdech, Z., Comparative  
15 959 gene expression profiling of *P. falciparum* malaria parasites exposed to three different histone  
16 960 deacetylase inhibitors. *PLoS one* **2012**, *7* (2), e31847.
- 17 961 60. Hansen, F. K.; Sumanadasa, S. D.; Stenzel, K.; Duffy, S.; Meister, S.; Marek, L.; Schmetter, R.;  
18 962 Kuna, K.; Hamacher, A.; Mordmuller, B.; Kassack, M. U.; Winzeler, E. A.; Avery, V. M.; Andrews, K. T.;  
19 963 Kurz, T., Discovery of HDAC inhibitors with potent activity against multiple malaria parasite life cycle  
20 964 stages. *European journal of medicinal chemistry* **2014**, *82*, 204-13.
- 21 965 61. Marfurt, J.; Chalfein, F.; Prayoga, P.; Wabiser, F.; Kenangalem, E.; Piera, K. A.; Fairlie, D. P.; Tjitra,  
22 966 E.; Anstey, N. M.; Andrews, K. T.; Price, R. N., Ex vivo activity of histone deacetylase inhibitors against  
23 967 multidrug-resistant clinical isolates of *Plasmodium falciparum* and *P. vivax*. *Antimicrobial agents and*  
24 968 *chemotherapy* **2011**, *55* (3), 961-6.
- 25 969 62. Sumanadasa, S. D.; Goodman, C. D.; Lucke, A. J.; Skinner-Adams, T.; Sahama, I.; Haque, A.; Do, T.  
26 970 A.; McFadden, G. I.; Fairlie, D. P.; Andrews, K. T., Antimalarial activity of the anticancer histone  
27 971 deacetylase inhibitor SB939. *Antimicrobial agents and chemotherapy* **2012**, *56* (7), 3849-56.
- 28 972 63. Trenholme, K.; Marek, L.; Duffy, S.; Pradel, G.; Fisher, G.; Hansen, F. K.; Skinner-Adams, T. S.;  
29 973 Butterworth, A.; Ngwa, C. J.; Moecking, J.; Goodman, C. D.; McFadden, G. I.; Sumanadasa, S. D.; Fairlie,  
30 974 D. P.; Avery, V. M.; Kurz, T.; Andrews, K. T., Lysine acetylation in sexual stage malaria parasites is a target  
31 975 for antimalarial small molecules. *Antimicrobial agents and chemotherapy* **2014**, *58* (7), 3666-78.
- 32 976 64. Salcedo-Amaya, A. M.; van Driel, M. A.; Alako, B. T.; Trelle, M. B.; van den Elzen, A. M.; Cohen, A.  
33 977 M.; Janssen-Megens, E. M.; van de Vegte-Bolmer, M.; Selzer, R. R.; Iniguez, A. L.; Green, R. D.;  
34 978 Sauerwein, R. W.; Jensen, O. N.; Stunnenberg, H. G., Dynamic histone H3 epigenome marking during the  
35 979 intraerythrocytic cycle of *Plasmodium falciparum*. *Proceedings of the National Academy of Sciences of*  
36 980 *the United States of America* **2009**, *106* (24), 9655-60.
- 37 981 65. Hoeijmakers, W. A.; Salcedo-Amaya, A. M.; Smits, A. H.; Francoijs, K. J.; Treeck, M.; Gilberger, T.  
38 982 W.; Stunnenberg, H. G.; Bartfai, R., H2A.Z/H2B.Z double-variant nucleosomes inhabit the AT-rich  
39 983 promoter regions of the *Plasmodium falciparum* genome. *Molecular microbiology* **2013**, *87* (5), 1061-73.
- 40 984 66. Coetzee, N.; Sidoli, S.; van Biljon, R.; Painter, H.; Llinas, M.; Garcia, B. A.; Birkholtz, L. M.,  
41 985 Quantitative chromatin proteomics reveals a dynamic histone post-translational modification landscape  
42 986 that defines asexual and sexual *Plasmodium falciparum* parasites. *Sci Rep* **2017**, *7* (1), 607.
- 43 987 67. Pinskaya, M.; Morillon, A., Histone H3 lysine 4 di-methylation: a novel mark for transcriptional  
44 988 fidelity? *Epigenetics* **2009**, *4* (5), 302-6.
- 45 989 68. Kafsack, B. F.; Rovira-Graells, N.; Clark, T. G.; Bancells, C.; Crowley, V. M.; Campino, S. G.;  
46 990 Williams, A. E.; Drought, L. G.; Kwiatkowski, D. P.; Baker, D. A.; Cortes, A.; Llinas, M., A transcriptional  
47 991 switch underlies commitment to sexual development in malaria parasites. *Nature* **2014**, *507* (7491), 248-  
48 992 52.
- 49 993 69. Jin, C.; Yang, L.; Xie, M.; Lin, C.; Merkurjev, D.; Yang, J. C.; Tanasa, B.; Oh, S.; Zhang, J.; Ohgi, K. A.;  
50 994 Zhou, H.; Li, W.; Evans, C. P.; Ding, S.; Rosenfeld, M. G., Chem-seq permits identification of genomic

- 995 targets of drugs against androgen receptor regulation selected by functional phenotypic screens.  
996 *Proceedings of the National Academy of Sciences of the United States of America* **2014**, *111* (25), 9235-  
997 40.
- 998 70. Zhang, X.; Huang, Y.; Shi, X., Emerging roles of lysine methylation on non-histone proteins. *Cell*  
999 *Mol Life Sci* **2015**, *72* (22), 4257-72.
- 1000 71. Iyer, L. M.; Abhiman, S.; de Souza, R. F.; Aravind, L., Origin and evolution of peptide-modifying  
1001 dioxygenases and identification of the wybutosine hydroxylase/hydroperoxidase. *Nucleic acids research*  
1002 **2010**, *38* (16), 5261-79.
- 1003 72. Markolovic, S.; Zhuang, Q.; Wilkins, S. E.; Eaton, C. D.; Abboud, M. I.; Katz, M. J.; McNeil, H. E.;  
1004 Lesniak, R. K.; Hall, C.; Struwe, W. B.; Konietzny, R.; Davis, S.; Yang, M.; Ge, W.; Benesch, J. L. P.; Kessler,  
1005 B. M.; Ratcliffe, P. J.; Cockman, M. E.; Fischer, R.; Wappner, P.; Chowdhury, R.; Coleman, M. L.; Schofield,  
1006 C. J., The Jumonji-C oxygenase JMJD7 catalyzes (3S)-lysyl hydroxylation of TRAFAC GTPases. *Nat Chem*  
1007 *Biol* **2018**, *14* (7), 688-695.
- 1008 73. Wilkins, S. E.; Islam, M. S.; Gannon, J. M.; Markolovic, S.; Hopkinson, R. J.; Ge, W.; Schofield, C. J.;  
1009 Chowdhury, R., JMJD5 is a human arginyl C-3 hydroxylase. *Nature communications* **2018**, *9* (1), 1180.
- 1010 74. Markolovic, S.; Wilkins, S. E.; Schofield, C. J., Protein Hydroxylation Catalyzed by 2-Oxoglutarate-  
1011 dependent Oxygenases. *The Journal of biological chemistry* **2015**, *290* (34), 20712-22.
- 1012 75. Trager, W.; Jensen, J. B., Continuous culture of *Plasmodium falciparum*: its impact on malaria  
1013 research. *Int J Parasitol* **1997**, *27* (9), 989-1006.
- 1014 76. McLean, K.; Straimer, J.; Hopp, C. S.; Vega-Rodriguez, J.; Tripathi, A.; Mlambo, G.; Doumolin, P.  
1015 C.; Harris, C. T.; Tong, X.; Shears, M. J.; Ankarklev, J.; Kafsak, B. F. C.; Fidock, D. A.; Sinnis, P., Generation  
1016 of Transgenic Human Malaria Parasites With Strong Fluorescence in the Transmission Stages. *bioRxiv*  
1017 **2018**.
- 1018 77. Fivelman, Q. L.; McRobert, L.; Sharp, S.; Taylor, C. J.; Saeed, M.; Swales, C. A.; Sutherland, C. J.;  
1019 Baker, D. A., Improved synchronous production of *Plasmodium falciparum* gametocytes in vitro.  
1020 *Molecular and biochemical parasitology* **2007**, *154* (1), 119-23.
- 1021 78. Grimberg, B. T., Methodology and application of flow cytometry for investigation of human  
1022 malaria parasites. *Journal of immunological methods* **2011**, *367* (1-2), 1-16.
- 1023 79. Muench, S. P.; Rafferty, J. B.; McLeod, R.; Rice, D. W.; Prigge, S. T., Expression, purification and  
1024 crystallization of the *Plasmodium falciparum* enoyl reductase. *Acta Crystallogr D Biol Crystallogr* **2003**,  
1025 *59* (Pt 7), 1246-8.
- 1026 80. Bhanu, N. V.; Sidoli, S.; Garcia, B. A., Histone modification profiling reveals differential signatures  
1027 associated with human embryonic stem cell self-renewal and differentiation. *Proteomics* **2016**, *16* (3),  
1028 448-58.
- 1029 81. Sidoli, S.; Bhanu, N. V.; Karch, K. R.; Wang, X.; Garcia, B. A., Complete Workflow for Analysis of  
1030 Histone Post-translational Modifications Using Bottom-up Mass Spectrometry: From Histone Extraction  
1031 to Data Analysis. *Journal of visualized experiments : JoVE* **2016**, (111).
- 1032 82. Robinson, M. D.; McCarthy, D. J.; Smyth, G. K., edgeR: a Bioconductor package for differential  
1033 expression analysis of digital gene expression data. *Bioinformatics (Oxford, England)* **2010**, *26* (1), 139-  
1034 40.
- 1035 83. McCarthy, D. J.; Chen, Y.; Smyth, G. K., Differential expression analysis of multifactor RNA-Seq  
1036 experiments with respect to biological variation. *Nucleic acids research* **2012**, *40* (10), 4288-97.
- 1037 84. Hulsen, T.; de Vlieg, J.; Alkema, W., BioVenn - a web application for the comparison and  
1038 visualization of biological lists using area-proportional Venn diagrams. *BMC genomics* **2008**, *9*, 488.

1039

1040 **For Table of Contents Use Only**